SAND2009-2694P

Finite Element Modeling of Complex Rheology

Rekha Rao

for

Lisa Mondy, David Noble, Sam Subia, Amy Sun, Matt Hopkins, Randy Schunk, Harry Moffat, Doug Adolf, Pin Yang

Sandia National Laboratories, Albuquerque, NM

Steve Altobelli

New Mexico Resonance, Albuquerque, NM

Randy Mrozek, Joe Lenhart

Army Research Laboratory, MD

Presented at
Procter and Gamble
West Chester, Ohio
May 21, 2009

Sandia is a multiprogram laboratory operated by Sandia Corporation, a Lockheed Martin Company, for the United States Department of Energy under contract DE-AC04-94AL85000.

GOMA MULTIPHYSICS CODE

A MP FINITE ELEMENT CODE FOR MULTIPHYSICS FREE AND MOVING BOUNDARY PROBLEMS

DELIVERY OF POLYMER/CERMET ENCAPSULANTS FOR MICRO ELECTRONICS AND NEUTRON GENERATOR PERFORMANCE AND RELIABILITY

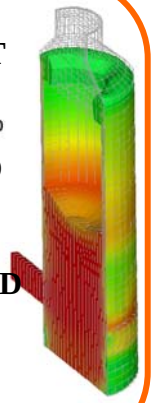

DP NG/NG TUBE FEED THROUGH

DP

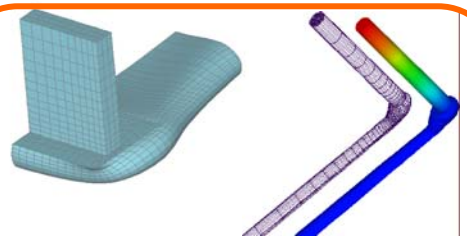

CERAMIC SLURRY EXTRUSION/RAPID PROTO FOR NG/ PZT APPS

MICROELECTRONICS AND MEMS-FLUIDICS MANUFACTURING AND PERFORMANCE – DP/ASCI

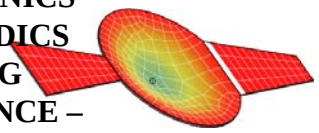

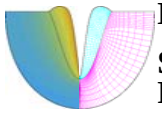

BRAZE/WELD/ SOLDER JOINT FORMATION - DP

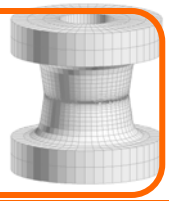

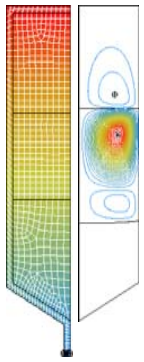

ALLOY PROCESSING **CRADA**

CORROSION/ELECTROCHEMICAL APPLICATIONS

PERFORMANCE, AGING AND RELIABILITY, LIGA

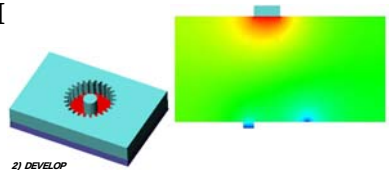

- **COUPLED OR SEPARATE HEAT, N-SPECIES, MOMENTUM (SOLID AND FLUID) TRANSPORT**
- **FULLY-COUPLED FREE AND MOVING BOUNDARY PARAMETERIZATION**
- **SOLIDIFCATION, PHASE-CHANGE, CONSOLIDATION, REACTION OF PURE AND BLENDED MATERIALS**
- **HOST OF MATERIAL MODELS FOR COMPLEX RHEOLOGICAL FLUIDS AND SOLIDS**

UNIQUE FEATURES MAKE GOMA IDEAL FOR MANUFACTURING PROCESSES IN WHICH

- **FREE SURFACES ARE UBIQUITOUS**
- **COUPLED FLUID-SOLID MECHANICS**
- **COMPLEX MATERIAL RHEOLOGY/LOW SPEED**
- **MULTIPHASE FLOW/POROELASTICITY**

COATING/ENCAPSULATION

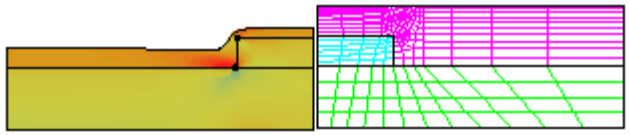

CRMPC CRADA/DP

GOMA: GENERAL MECHANICS CAPABILITIES

- **MATERIAL MODELS, SOLIDS**

  ELASTICITY (LINEAR, NONLINEAR, INCOMPRESSIBLE); ELASTOVISCOPLASTICITY WITH SPECIES TRANSPORT; POROELASTICITY;

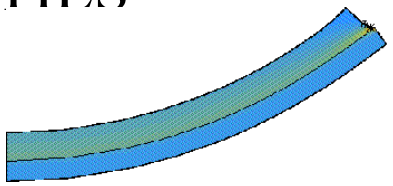

- **MATERIAL MODELS, FLUIDS**

  NEWTONIAN; GENERALIZED NEWTONIAN; MULTIMODE VISCOELASTICITY; CONTINUUM SUSPENSION MODEL;

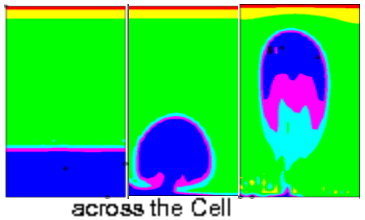

- **SPECIES TRANSPORT MODELS/PHYSICS**

  FICKIAN; NON-FICKIAN, MULTICOMPONENT; CHARGED SPECIES; FREE VOLUME THEORY;

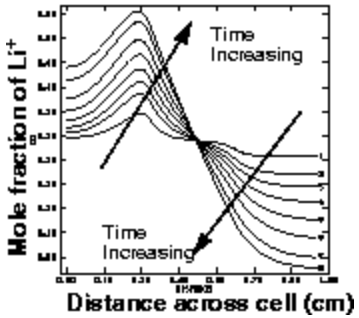

- **PHASE CHANGE AND INTERFACIAL PHYSICS**

  IDEAL AND NONIDEAL VAPOR-LIQUID EQUILIBRIUM; VAPOR PRESSURE MODELS FOR IDEAL, NONIDEAL AND MICROPOROUS SYSTEMS; LIQUID-SOLID PHASE CHANGE (LATENT HEAT RELEASE AT LAGRANGIAN OR EULERIAN INTERFACES); MACROSEGREGATION MODELS

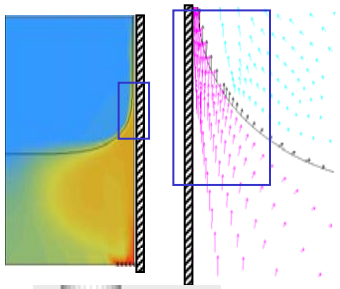

- **SPECIAL FLUID-SOLID, FLUID-STRUCTURE CONDITIONS**

- **PARTICLE-FLUID PHYSICS**

  DISCRETE PARTICLE-CONTINUUM FLUID COUPLING

- **SPECIALIZED SHELL ELEMENT CAPABILITIES**

  STRUCTURAL SHELLS (MEMBRANES); FLUID SHELLS (LUBRICATION)

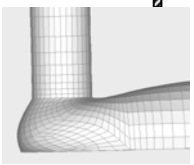

RHEOLOGICAL MODELS CURRENTLY IN GOMA

Generalized Newtonian models (concentration, temperature and shear-rate dependence)

- **Carreau**
- **Carreau-WLF**
- **Molten glass**
- **Curing epoxy**
- **Bingham-plastic**

Augmented Generalized Newtonian Models (include evolution equations for particle concentration)

- **Modified Phillips**
- **Suspension Balance**

Multimode viscoelastic history dependent models

- **Maxwell/Oldroyd-B**
- **Phan-Thien Tanner**
- **Giesekus**

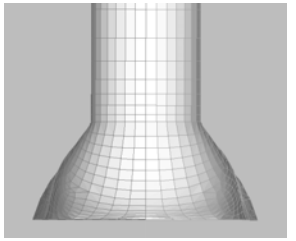

Extrusion

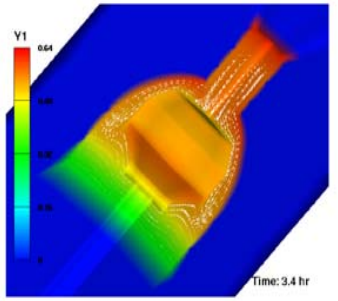

Curing and settling of a particle-filled epoxy in a mold

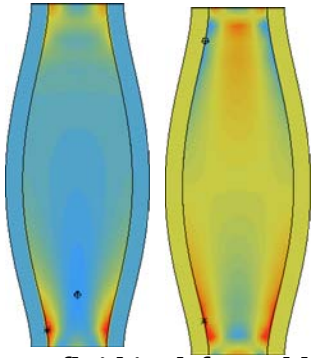

VE fluid in deformable tube

Complex material model expertise spans a wide range of behaviors

Embedded Interface Methods Can Capture Topological Changes

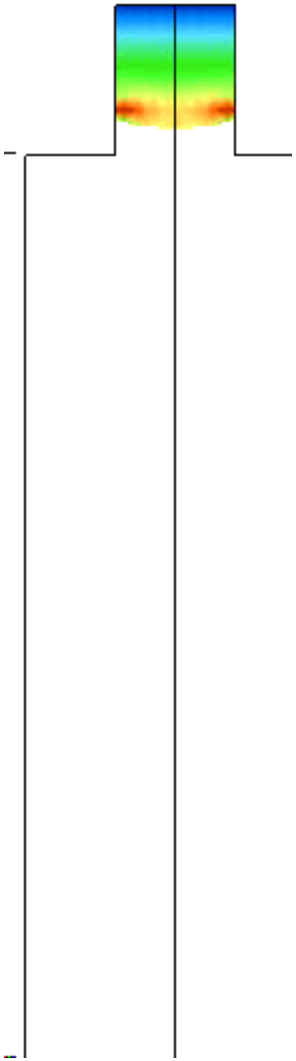

- Level set method has possibility of modeling "Dairy Queen" effect

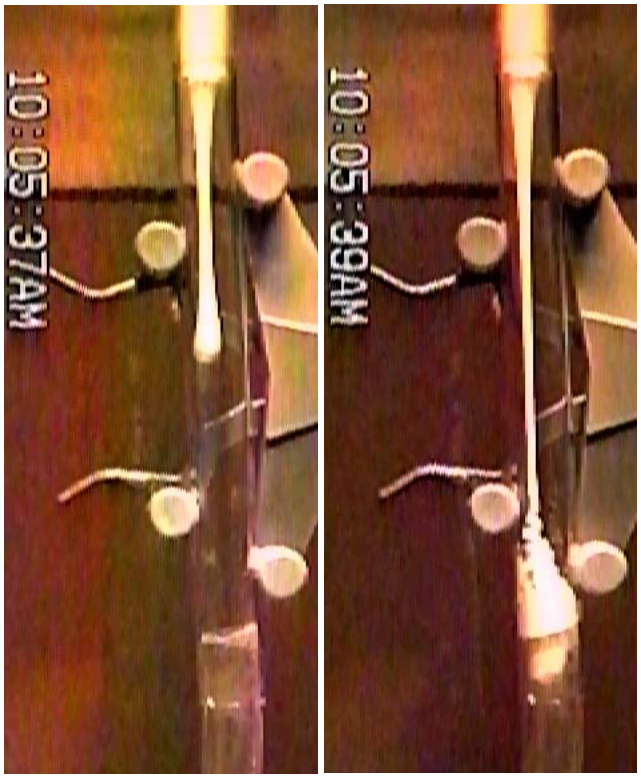

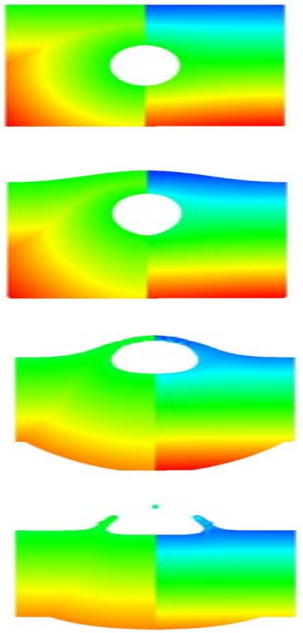

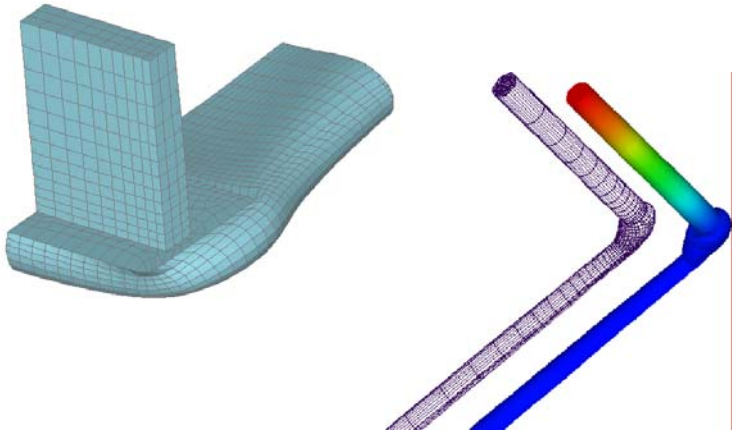

Numerical Solution Methods for Interfacial Motion

Tracking motion of interface between two distinct phases appears often:

- Phase changes
- Film growth
- Fluid filling

Interface tracking:

- Explicit parameterization of location
- Interface physics more accurate
- Moving mesh
- Limits to interface deformation
- No topological changes

Examples:

Spine methods (*Scriven*)

ALE

Embedded Interface Capturing:

- Interface reconstructed from higher dimensional function
- Fixed mesh
- "Diffuse" interface physics
- Interface deformation theoretically unconstrained

Examples:

Volume-of-Fluid (*Hirt*)

Level Sets (*Sethian*)

Finite Element Implementation

- **Approximate variables with trial function, e.g.**

$$u \approx \sum_{i=1}^{n} u_i N_i \quad v \approx \sum_{i=1}^{n} v_i N_i \quad w \approx \sum_{i=1}^{n} w_i N_i \quad p \approx \sum_{i=1}^{m} p_i N_i^{'}$$

- **Substitute into equations of motion, weight residual with shape function for Galerkin implementation**

$$Weighted\text{-}Residual = \int N_i R_i dV$$

- **Gaussian quadrature**
- **Solve discretized system**

$$\underline{\underline{A}}\,\underline{x} = \underline{b}$$

- **Issues: Linear system solved with Krylov-Based iterative solvers => require stabilization**

Sandia National Laboratories

Discretization Method for 3D Level Set Problems

- Formulation uses a coupled u-p solve with a decoupled level set solve
- Direct Gaussian elimination solvers are not feasible for 3D – bandwidth and scalability issues
- Stabilized methods must be used to obtain large 3D solutions with Krylov-based iterative solver
- Stabilized methods that may work well on single phase flows, have difficulty handling the pressure jumps associated with the level set method
- Mass loss issues associated with pressure jumps have hampered progress

Massively Parallel Implementation

Free Surface Flows: Coupling Fluid Flow to Pseudo-Solid Mesh Motion

- Technique for mapping mesh nodes in response to boundary deformation
- Displacement of nodes determined by solution of quasi-static problem:

$$\nabla \cdot \mathsf{T}_{mesh} = 0, \quad \mathsf{T}_{mesh} = f(\lambda_{ps}, \mu_{ps}; \nabla d_{mesh})$$

- Mesh node displacements are solved for simultaneously with other variables
- Deformation driven by boundary constraints:

Geometric

$$P(x,y,z) = 0$$

$$\vec{d} = \vec{D}_0$$

$$n_1 \cdot n_2 = \cos(\theta)$$

Coupled

$$n \cdot v = 0$$

$$T = T_{melt}$$

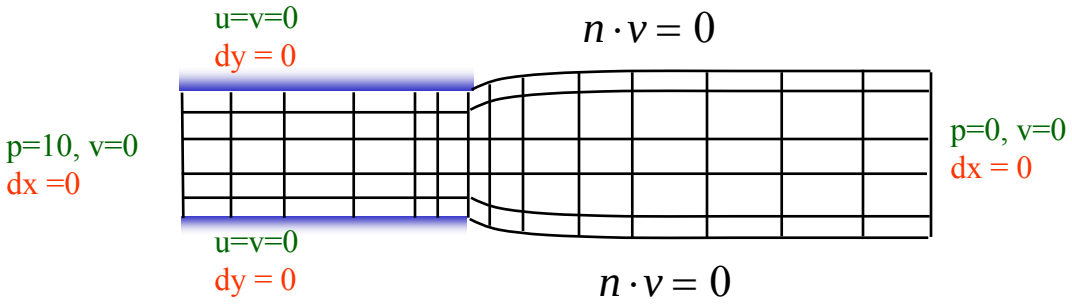

Arbitrary Lagrangian Eulerian (ALE) mesh motion: The mesh moves with the material at boundaries and arbitrarily, as a nonlinear elastic solid, elsewhere.

Sackinger, Schunk, and Rao, 1994; Cairncross et al, 2000; Baer et al, 2000

Basics of Level Set Method

The level set function, $\phi(x,y,z)$ is the representing function

- Signed minimum distance to the interfacial curve
- Sign of ϕ distinguishes phase physics.
- The contour $\phi(x,y,z) = 0$ “represents” the interface <u>when needed</u>
- Evolution of $\phi(x,y,z)$ such that $\phi(x,y,z) = 0$ remains on the interface

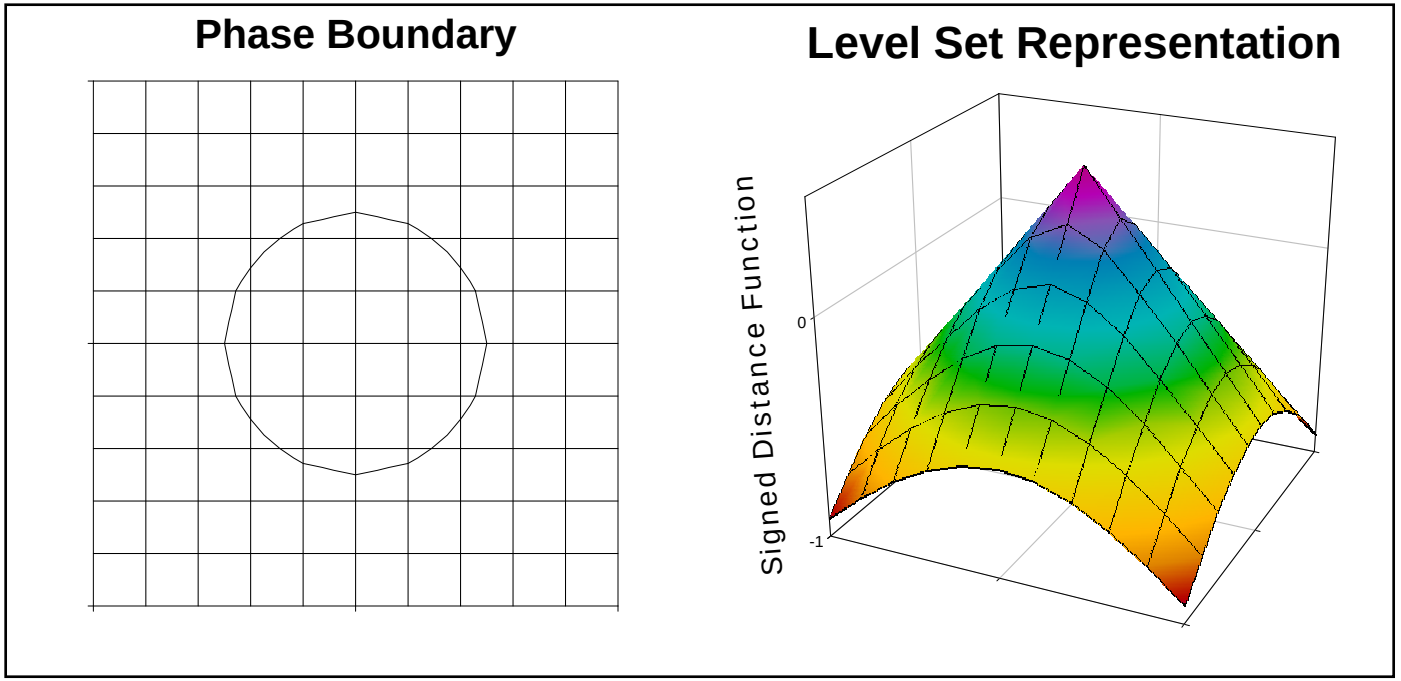

Free Surface Flow: Level Set Method

Given fluid velocity field, u(x,y,z), evolution on a fixed mesh is according to:

$$\frac{\partial \phi}{\partial t} + u \cdot \nabla \phi = 0 \qquad \vec{n} = \nabla \phi, \kappa = \nabla \cdot \nabla \phi$$

Purely hyperbolic equation … fluid particles on $\phi(x,y,z) = 0$ should stay on this contour indefinitely

- Does not preserve $\phi(x,y,z)$ as a distance function
- Introduces renormalization step.

Fluid velocity evolves as one-phase fluid with properties that depend on ϕ

$$\rho(\varphi)\frac{Du}{Dt} = -\nabla P + \nabla \cdot (\mu(\varphi)\dot{\gamma}) + \rho(\varphi)g + I.T., \quad \nabla \cdot u = -\frac{D\rho(\varphi)}{Dt}$$

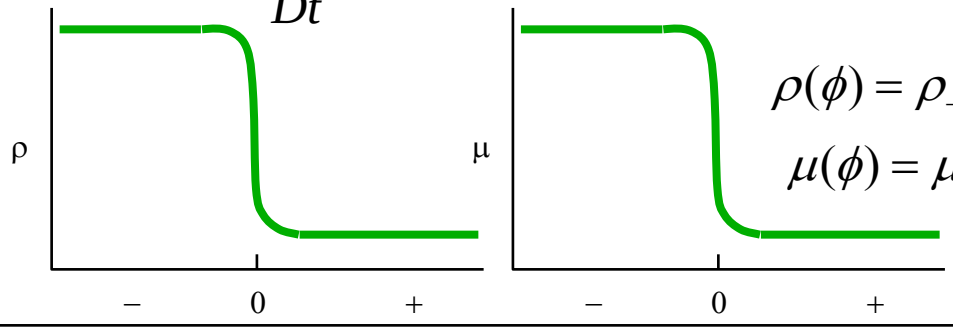

$$\rho(\phi) = \rho_{-}(1 - H_{\alpha}(\phi)) + \rho_{+}H_{\alpha}(\phi)$$

$$\mu(\phi) = \mu_{-}(1 - H_{\alpha}(\phi)) + \mu_{+}H_{\alpha}(\phi)$$

$$\underline{T_{\sigma}} = \sigma\delta_{\alpha}(F)\left(\underline{I} - \vec{n}\vec{n}\right)$$

Sandia National Laboratories

Motivation: Foam Processing

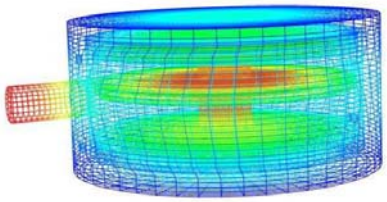

Thermal modeling of mock AFS

Mixing protocols change foam density and microstructure

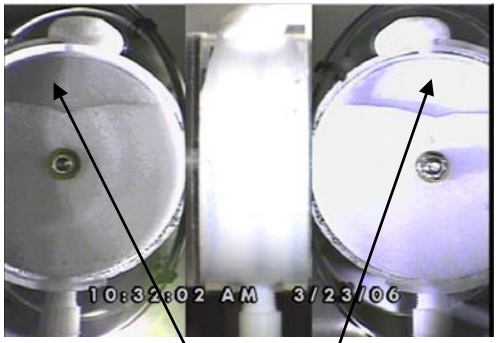

Flow visualization shows voids

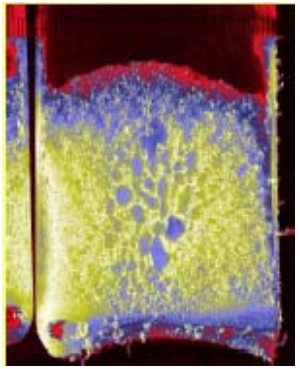

NMR imaging shows coarse microstructure (Altobelli, 2006)

Problem Description:

- Electronic components are encapsulated with blown foams
- Foam materials critical for structural support and shock/vibration isolation
- Foaming can be unpredictable leading to unacceptable voids
- Inhomogeneities in foam material can lead to property variations & potential structural issues
- Foam self-expansion dynamics very different from pressure driven flow

Foam process models can be used to improve mold design, optimize vent/gate locations, decrease defects, and trouble shoot issues

Sandia National Laboratories

Foam of Interest is Physically Blown Epoxy Foam

Vision: Develop a continuum model with volume source terms, and include relevant physics in these terms. Single phase, homogenized model

Process

- Two part epoxy, starts as an emulsion
  - Part B (shaken to distribute components)
    - Cabosil M-5 (particulate for nucleation sites)
    - curing agent
    - surfactant
    - FC-72 Fluorinert (blowing agent immiscible with curing agent)
  - Mixed with Part A, the resin
- Foam is blown by heating
  - 65^{o}C oven (FC-72 boils at 53^{o}C)

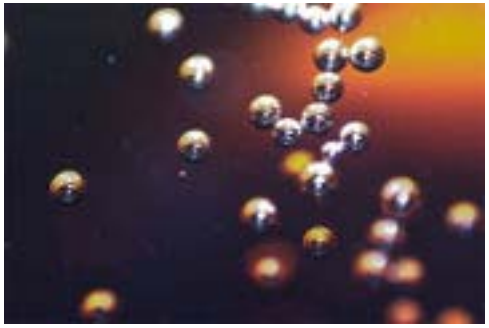

Bubbles in a soft drink nucleate homogenously, responding to a decrease in pressure

Coupled Computational Modeling

- Model development closely linked to experimental work
  - Experimental discovery
  - Parameter estimation
  - Validation experiments
- Kinetics of polymerization
- Rheology
- Blowing agent transport, nucleation, and growth
- Thermal/Fluid mechanics
- Free surface flow

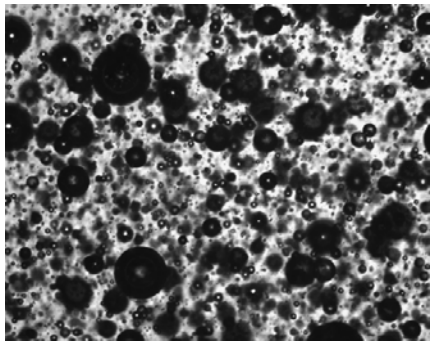

Epoxy foam starts out as an emulsion and probably nucleates heterogeneously

Sandia National Laboratories

Level Set Model Improves Understanding of Foam Self-Expansion

$$\rho\frac{\partial \mathbf{v}}{\partial t} = -\rho\mathbf{v}\bullet\nabla\mathbf{v} - \nabla p + \mu_f\nabla^2\mathbf{v}$$

$$\nabla\bullet\mathbf{v} = -\frac{1}{\rho_f}\frac{\partial\rho_f}{\partial t}$$

$$\rho = \rho_{final} + (\rho_{initial} - \rho_{final})e^{-kt}$$

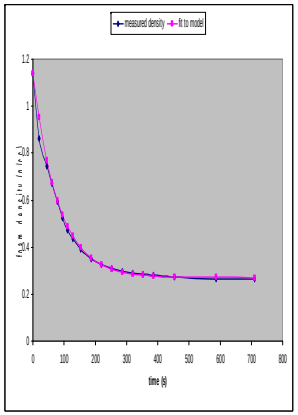

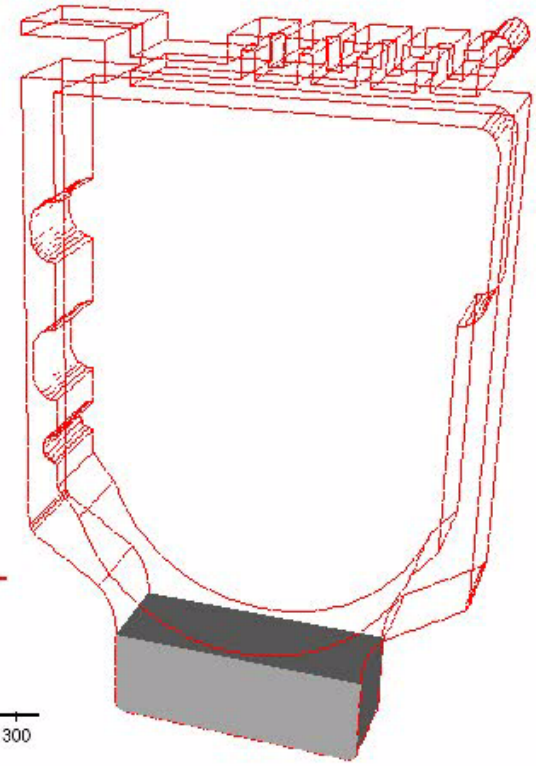

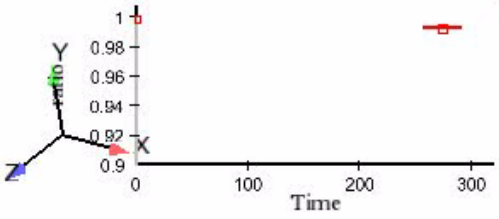

- Equations of motion are coupled to a time dependent density function fit from experimental data for EFAR20 foam
- Foam is assumed Newtonian and isothermal
- Location of the free surface with time is determined from the zero of the level set equation
- Methodology can be applied to other foams

D. Seo; J. R. Youn; C.L.I. Tucker *IJNMF*, 2003

Sandia National Laboratories

Comparison of Simulations to Validation Data: Isothermal Model

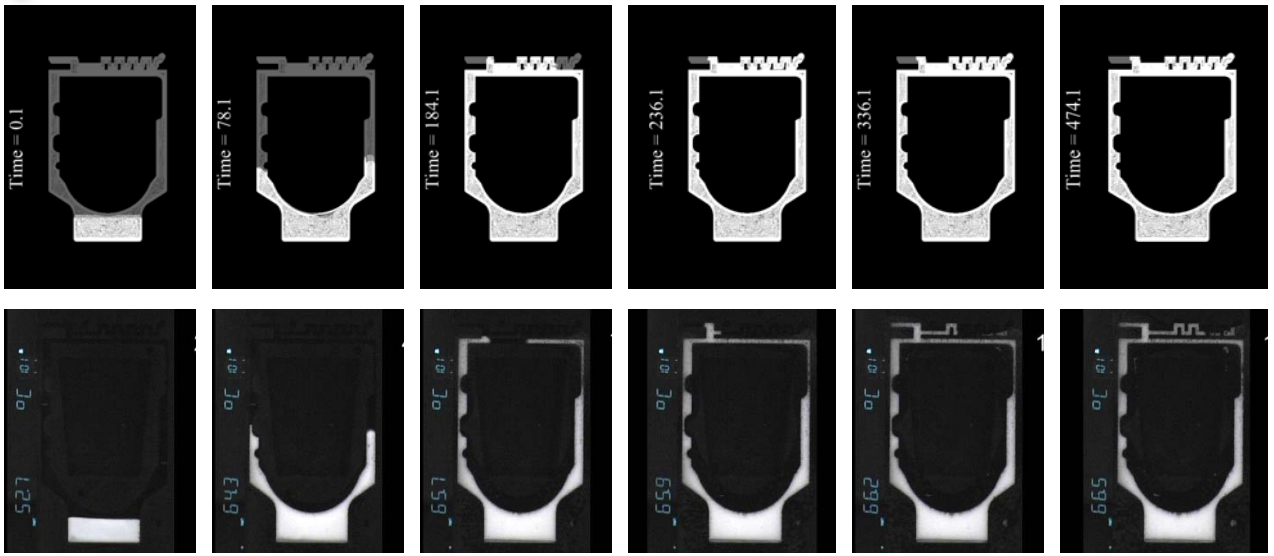

T=0s T=78.6s T=184.1s T=236.4s T=337.1s T=474.0s

Volume vs time plot shows good match between data and simulation => Model more than adequate for engineering analysis

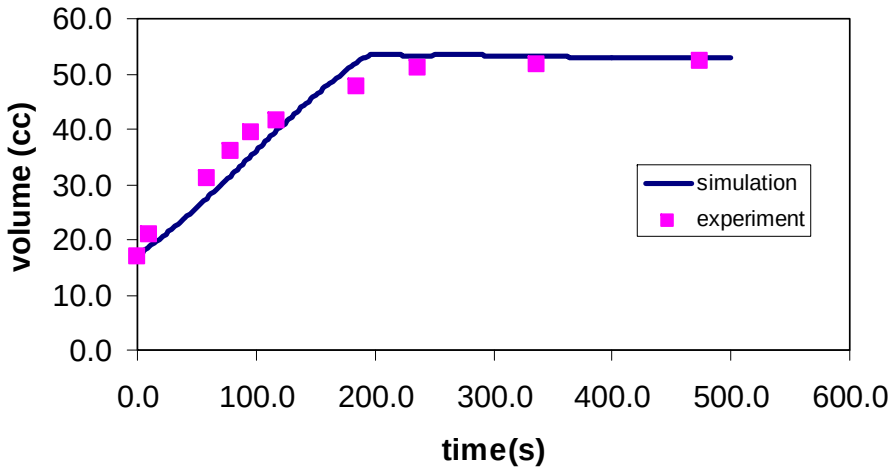

- Finite element/level set isothermal model assuming a time-dependent density function measured from foam rise experiments in a different geometry
- Validation experiments show some foam leakage ahead of the front, void trapped in upper left hand corner escapes the mold
- Experiments were purposefully under-filled so we could determine final volume
- Simulations fill faster than experiments, especially in small features where bubbles show noncontinuum behavior

Sandia National Laboratories

Reaction Kinetics and Rheology for Continuous Phase Determined Experimentally

- Reaction kinetics for foam determined by differential scanning calorimetry
- Polymerization of epoxy material follows condensation chemistry
- Reaction is exothermic (ΔH_{rxn} = 250 J/g)
- Heat produced drives the reaction faster
- k=1.145e5 ΔE=10kcal/mol, n=1.3

$$\frac{d\xi}{dt} = ke^{\Delta E/RT}(1-\xi)^n$$

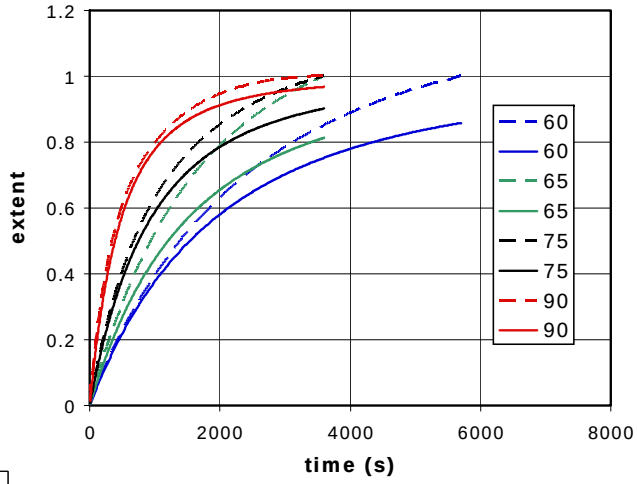

- Viscosity increases with cure
- Correlate viscosity with extent of reaction

$$\mu_0 = \mu_0^0 \exp\left(\frac{E_\mu}{RT}\right)\left(\frac{\xi_c^{\,2} - \xi^2}{\xi_c^2}\right)^{-4/3}$$

- Viscosities are a function of void fraction (Taylor-Mooney)

$$\mu = \mu_0 \exp\left(\frac{\phi_{gas}}{1-\phi_{gas}}\right)$$

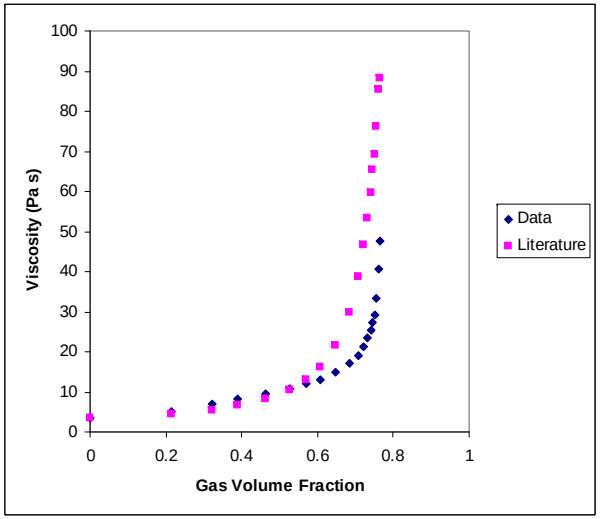

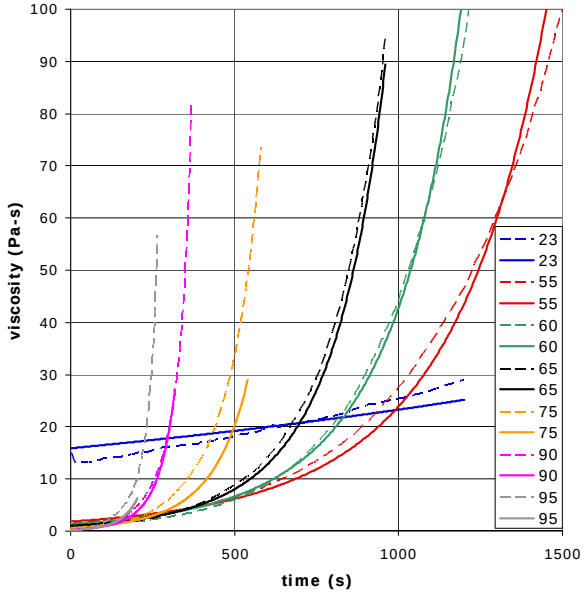

$$\lambda = \frac{4}{3}\mu_0 \frac{(\varphi_{gas} - 1)}{\varphi_{gas}}$$

Sandia National Laboratories

Higher Fidelity Model Adds More Complex Material Models with Cure, Temperature, and Void Fraction Dependence

$$\rho\frac{\partial \mathbf{v}}{\partial t} = -\rho\mathbf{v}\bullet\nabla\mathbf{v} - \nabla p + \nabla\bullet(\mu_f(\nabla\mathbf{v} + \nabla\mathbf{v}^t)) - \nabla\bullet\lambda(\nabla\bullet\mathbf{v})I + \rho\mathbf{g}$$

$$\rho C_{pf}\frac{\partial T}{\partial t} + \rho C_{pf} v\bullet\nabla T = \nabla\bullet(k\nabla T) + \rho\phi_e\Delta H_{rxn}\frac{\partial\xi}{\partial t} - \rho\lambda_{evap}\frac{\partial\phi_l}{\partial t}$$

$$\nabla\bullet\mathbf{v} = -\frac{1}{\rho_f}\left(\frac{\partial\rho_f}{\partial t} + \mathbf{v}\bullet\nabla\rho_f\right)$$

$$\frac{\partial\xi}{\partial t} + \nabla\bullet(\xi v) = k^i e^{\Delta E/RT}(1-\xi)^n$$

$$\rho = \rho_{final} + (\rho_{initial} - \rho_{final})e^{-at} \qquad \text{a=f(T)}$$

$$\mu = \mu_0\exp\left(\frac{\varphi_v}{1-\varphi_v}\right) \quad \mu_0 = \mu_0^0\exp\left(\frac{E_\mu}{RT}\right)\left(\frac{\xi_c^{\,2} - \xi^2}{\xi_c^2}\right)^{-4/3}$$

$$\lambda = \frac{4}{3}\mu_0\frac{(\phi_v - 1)}{\phi_v}$$

$$k = \frac{2}{3}\left(\frac{\rho}{\rho_e}\right)k_e + \left(1 - \frac{\rho}{\rho_e}\right)k_v$$

$$C_{pf} = C_{pl}\phi_l + C_{pv}\phi_v + C_{pe}\phi_e$$

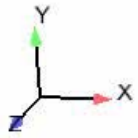

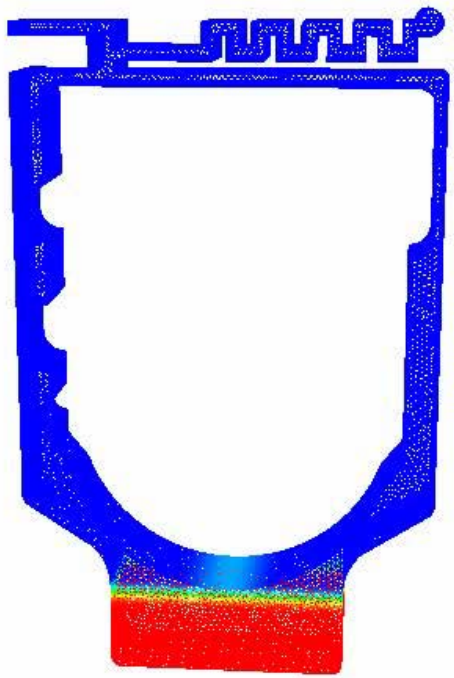

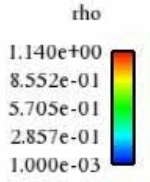

Time scale and filling behavior set by density equation and unaffected by increasing shear viscosity or dilatational effects

Sandia National Laboratories

Comparison of Simulation to Experiment

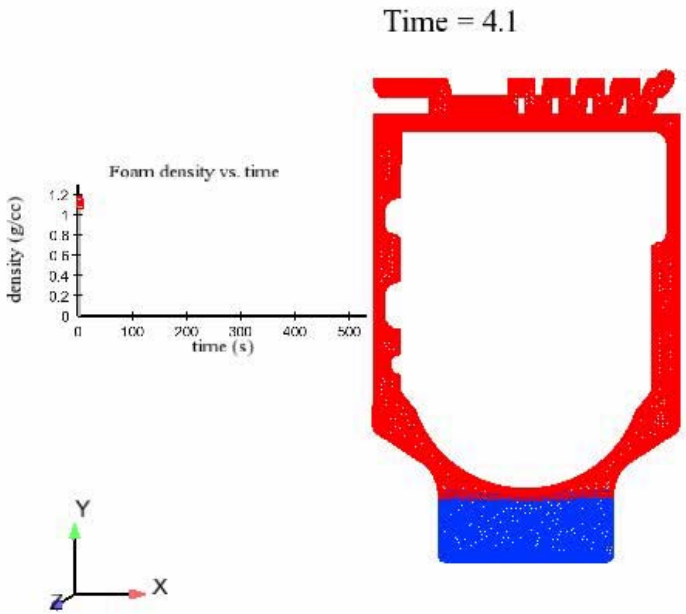

- Simulation uses curing viscosity without volume fraction effects or bulk viscosity
- Thermal effects are included
- Homogeneous time and temperature dependent density
- Void is trapped in upper left hand corner where fluid reaches a dead end

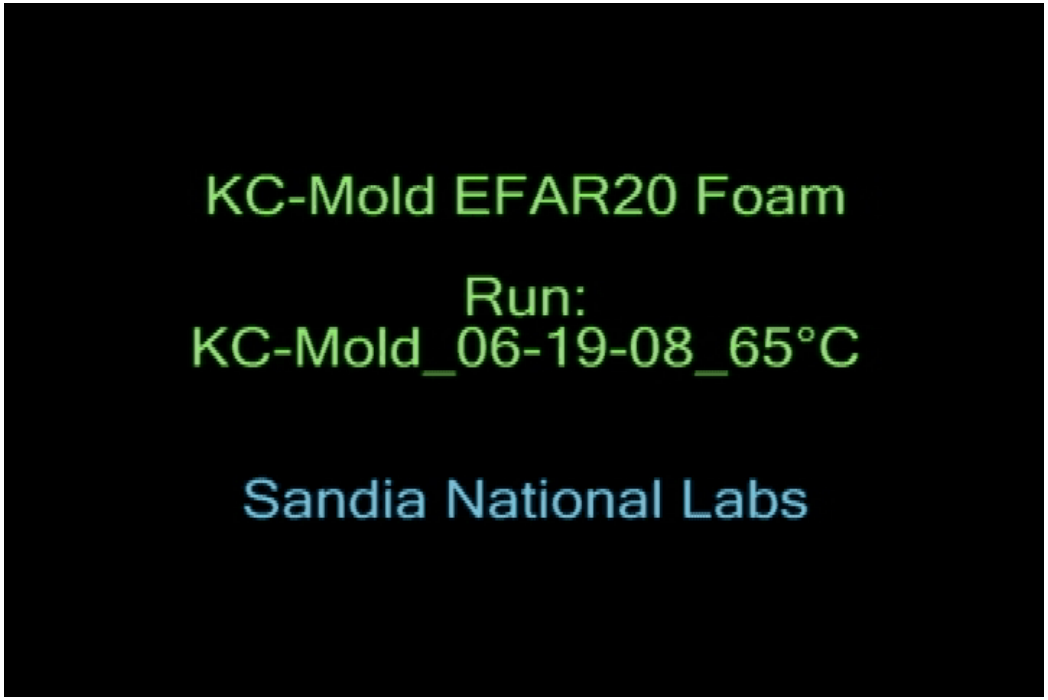

- Flow visualization shows non-continuum effects in thin channel where bubbles the size of the channel move with a pulsatile motion
- Void is trapped in upper left hand corner but air diffuse away either into foam or out the face plate

Sandia National Laboratories

Thermal Properties Vary with Gas Volume Fraction while Viscosities Vary also with Temperature and Cure

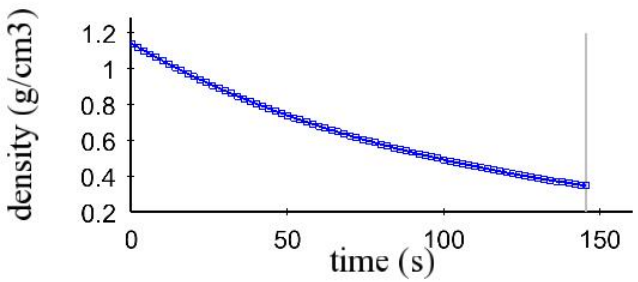

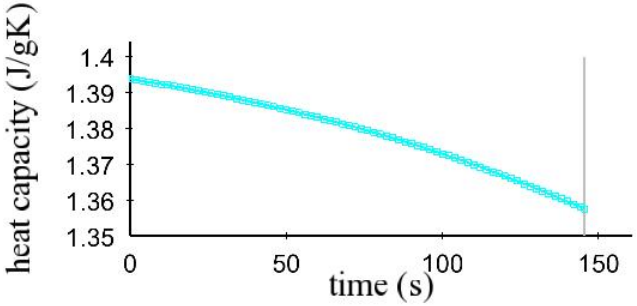

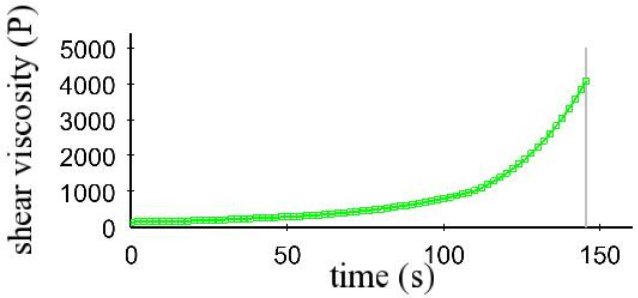

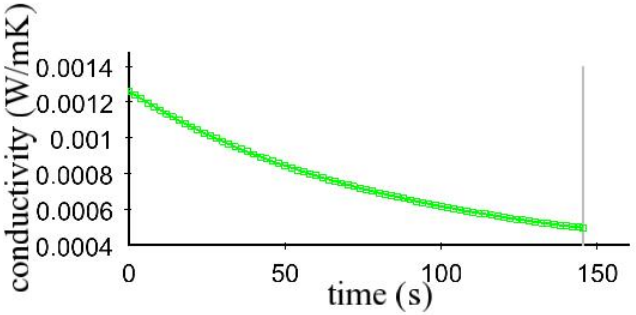

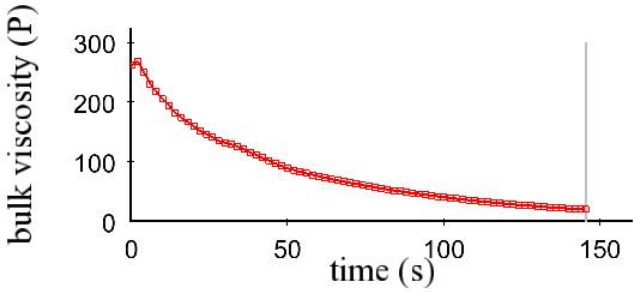

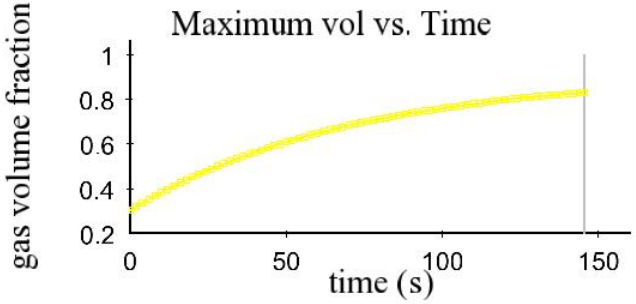

Sandia National Laboratories

Thermal Model Validation for Full Model: Two Different Temperature Initial Condition

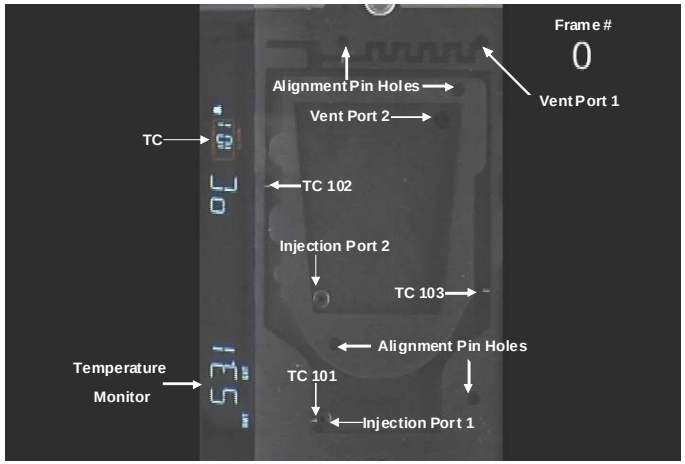

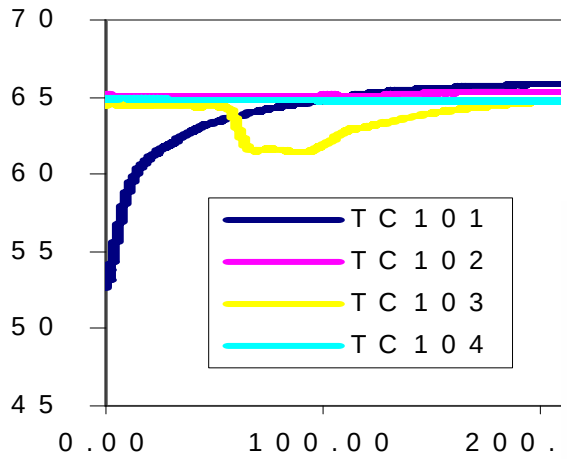

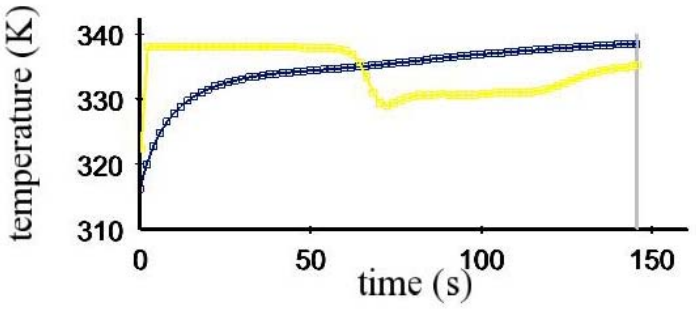

$T_{initial} = 43^{o}C$

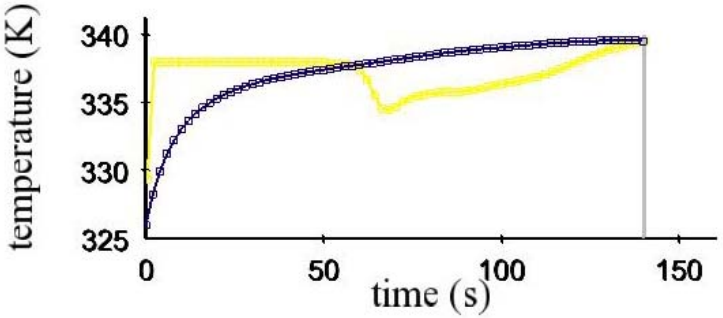

$T_{initial} = 52.7^{o}C$

For future work, we would like to look at the temperature at the cooler spots in the mo

Sandia National Laboratories

Density Gradients Motivate Current Work: Including Localized Bubble Buoyancy Effects

Oven temperature = 65 C

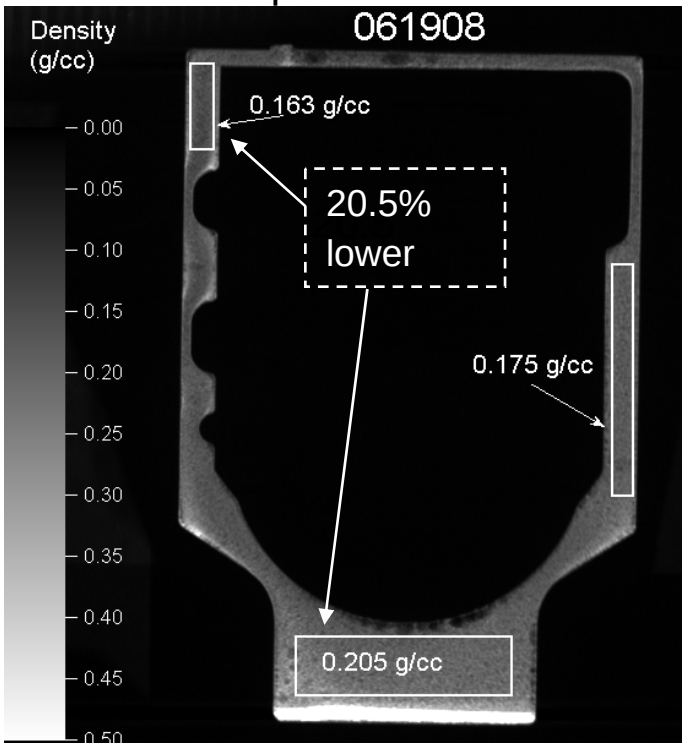

Thompson, 2008

- Fluorinert blowing agent forms into droplets in mixing process
- Single droplet in mix will superheat without boiling – no boiling at typical oven temperatures
- Only "blows" when interacts with a bubble
- Droplet Rd ~ 10 μm and air bubble R_b ~ 100μm gives an average collision time on the order of minutes if Δx is on the order of 100μm.
- Explains why final foam density is dependent on mixing procedure – must incorporate air and have optimal droplet/bubble sizes

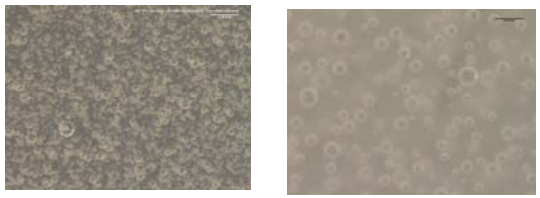

Mixing study (KCP): Left, "sweet spot" for good foam rise is between 800 and 1300 rpm. Right, foam rises only poorly when malt mixer at about 10,000 rpm is used.

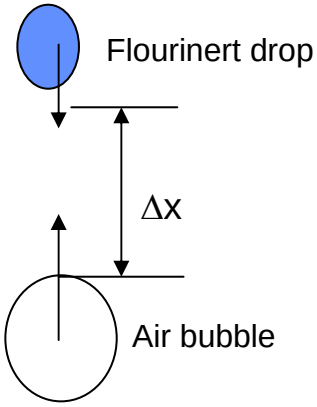

- Density variations range from unfoamed (1 g/cc) to foamed (0.2 g/cc), with foamed part varying approximately another 20%

Sandia National Laboratories

Suspension rheology complicated by particle migration

NMR IMAGING EXPERIMENTS

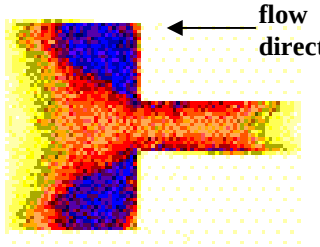

Particle preferentially migrate to center of pipe

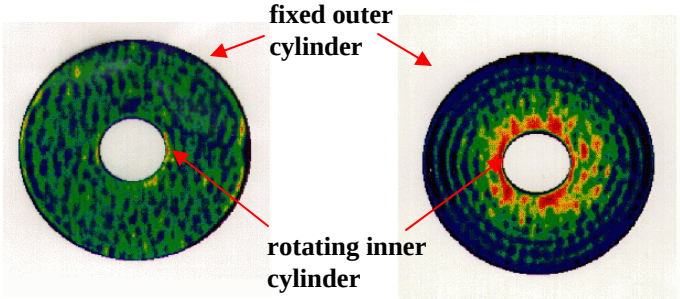

initially well-mixed

after 50 turns of inner cylinder

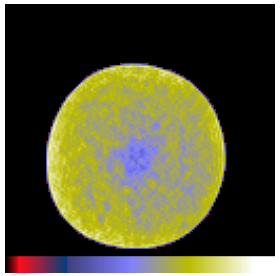

near inline mixer

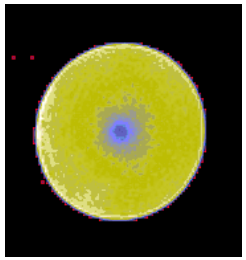

steady state profile

During flow, migration of particles creates inhomogeneities that cannot be described by a constant Newtonian viscosity

Expansion Flow

Fluid rich region appears at corners of large pipe as particles are swept out (Mondy et al., 1995)

Concentric Couette

Particles move away from inner cylinder (Graham et al., 1991)

Pipe Flow

Particles migrate toward the center of the pipe (Hampton et al., 1997)

Particles migrate from regions of high shear-rate to low, from high concentration to low and from high relative viscosity to low (Leighton and Acrivos, 1987)

Modeling Suspension Flow with a Continuum Constitutive Equation

Momentum equation has a non-Newtonian viscosity dependent on local particle concentration (Krieger model)

$$\rho\frac{\partial v}{\partial t}+\rho v\bullet\nabla v=-\nabla p+\nabla\bullet\left(\eta\left(\nabla v+\nabla v^{t}\right)\right)$$

$$\nabla\bullet v=0$$

Evolution equation describing particle migration

$$\frac{\partial\phi}{\partial t}+v\bullet\nabla\phi=-\frac{\nabla\bullet J_{s}}{\rho}$$

$$\frac{J_{s}}{\rho}=-\left(\phi K_{c}\nabla(\dot{\gamma}\phi)+\phi^{2}\dot{\gamma}K_{\eta}\nabla(\ln\eta)\right)$$

K_c and K_η are coefficients that must be fit to data. They are on the order of the particle size squared

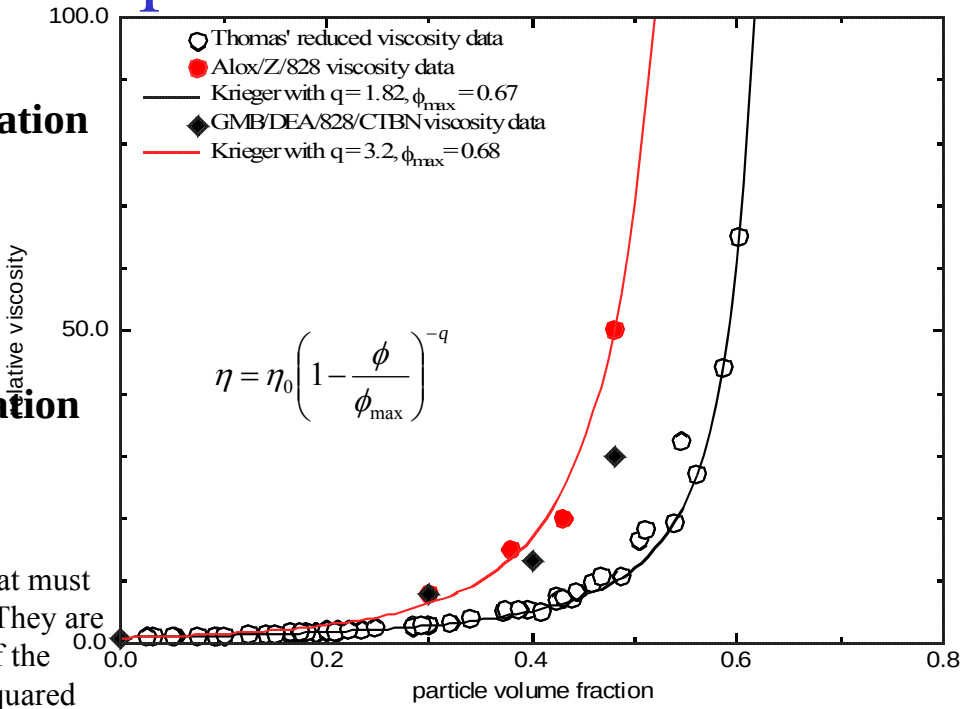

Assumptions

- particle migration depends on shear-rate invariant, particle volume fraction and suspension viscosity (Phillips et al., 1992)
- particles and fluid have same velocity
- neutrally buoyant particles
- Spherical monodisperse particles
- enough particles to establish a continuum
- particles are larger than 10 μm
- no colloidal effects
- no electrostatic forces
- Newtonian suspending fluid

Suspension Flow: Neutrally Buoyant Particles

Continuum finite element modeling agrees well with NMR data for large, uniform spheres that are neutrally buoyant in Newtonian oil.

- **Extent of migration**
- **Rate of particle migration**
- **Asymmetry**

Must extend model for non-neutrally buoyant particles in non-Newtonian or polymerizing media for our applications

- **settling/floating particles such as alumina and glass microballoons (GMB)**
- **epoxy cures dramatically changing suspending fluid viscosity**
- **Non-Newtonian suspending fluids**

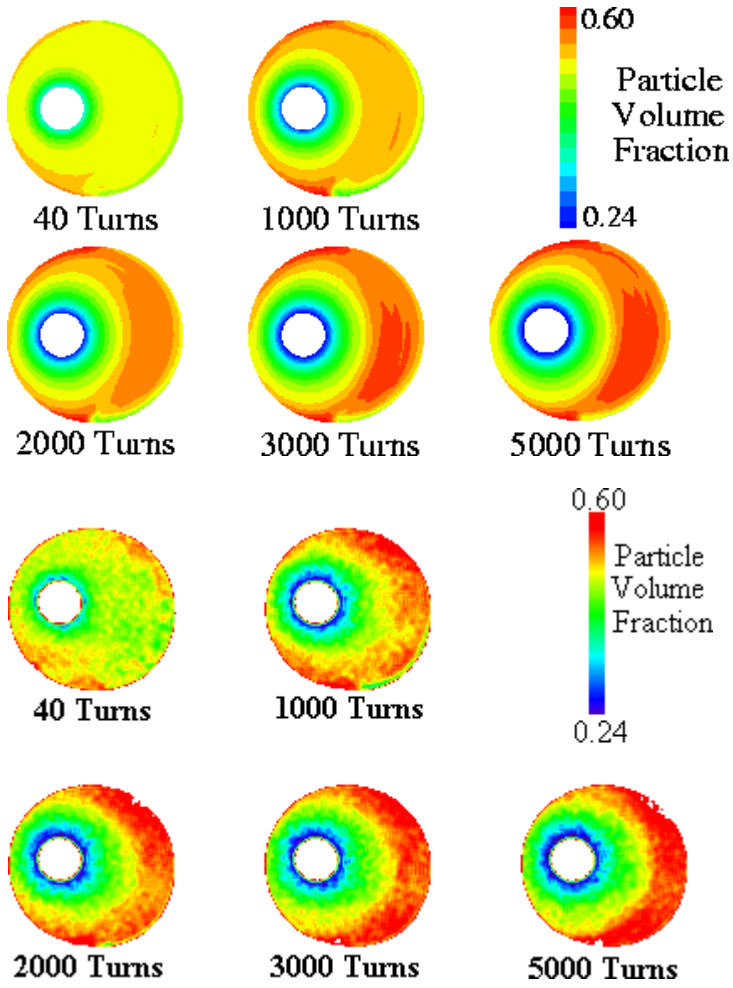

Extension of Diffusive Flux Model for Buoyant Particles (Zhang and Acrivos, 1994)

Flow field becomes much more complex with the introduction of divergent non-Newtonian viscosity, viscous resuspension and particle settling. Secondary flows are common. For neutrally buoyant particles, Couette simulation would be one dimensional.

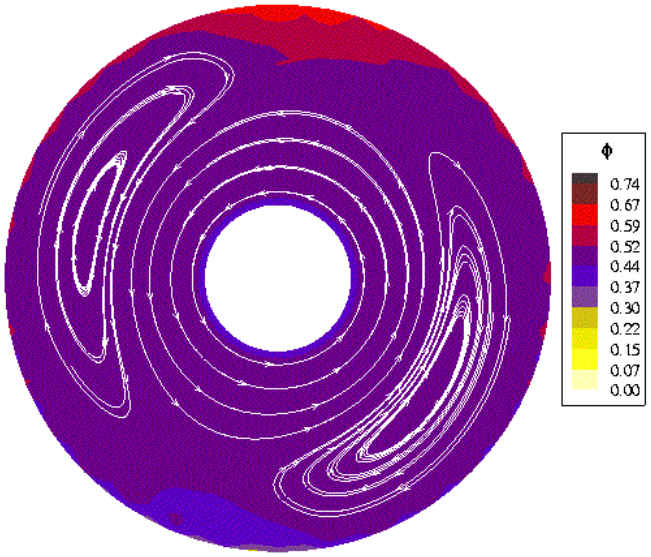

Couette Simulation

$$\rho\frac{\partial v}{\partial t}+\rho\boldsymbol{v}\bullet\nabla\boldsymbol{v}+\nabla p-\nabla\bullet\left(\eta\left(\nabla\boldsymbol{v}+\nabla\boldsymbol{v}^{T}\right)\right)-\left(\rho_{f}-\rho_{s}\right)\phi g=0$$

$$\rho=\left(1-\phi\right)\rho_{f}+\phi\rho_{s}\qquad\eta=\eta_{0}\left(1-\frac{\phi}{\phi_{m}}\right)^{-n}$$

$$\frac{\partial\phi}{\partial t}+\nabla\bullet\left(\phi\boldsymbol{v}\right)=\frac{\nabla\bullet J_{s}}{\rho_{s}}$$

$$\frac{J_{s}}{\rho_{s}}=-\left(\phi K_{c}\nabla\left(\dot{\gamma}\phi\right)+\phi^{2}\dot{\gamma}K_{\eta}\nabla\left(\ln\eta\right)\right)+f_{hindered}v_{stokes}\phi$$

$$\nabla\bullet\boldsymbol{v}=\frac{\left(\rho_{f}-\rho_{s}\right)}{\rho_{s}\rho_{f}}\nabla\bullet J_{s}$$

- **For suspension, particles and suspending fluid have different densities, so velocity field is no longer solenoidal**
- **Suspension can exhibit solid-like behavior once particles reach maximum packing concentration**
- **Choice of hindered settling function can effect results (Richardson-Zaki, Acrivos, …)**

Quiescent Settling in a Contracted Cylinder

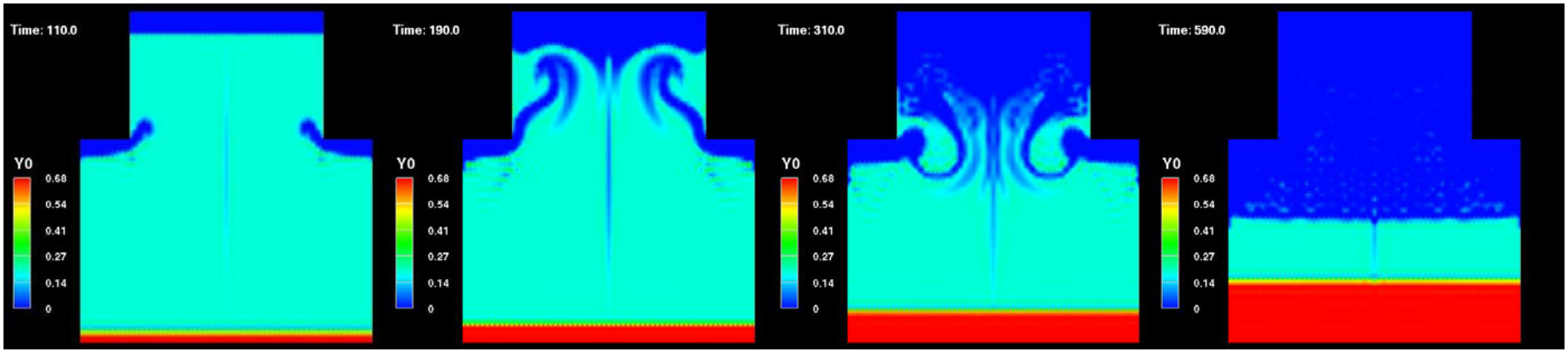

simulation

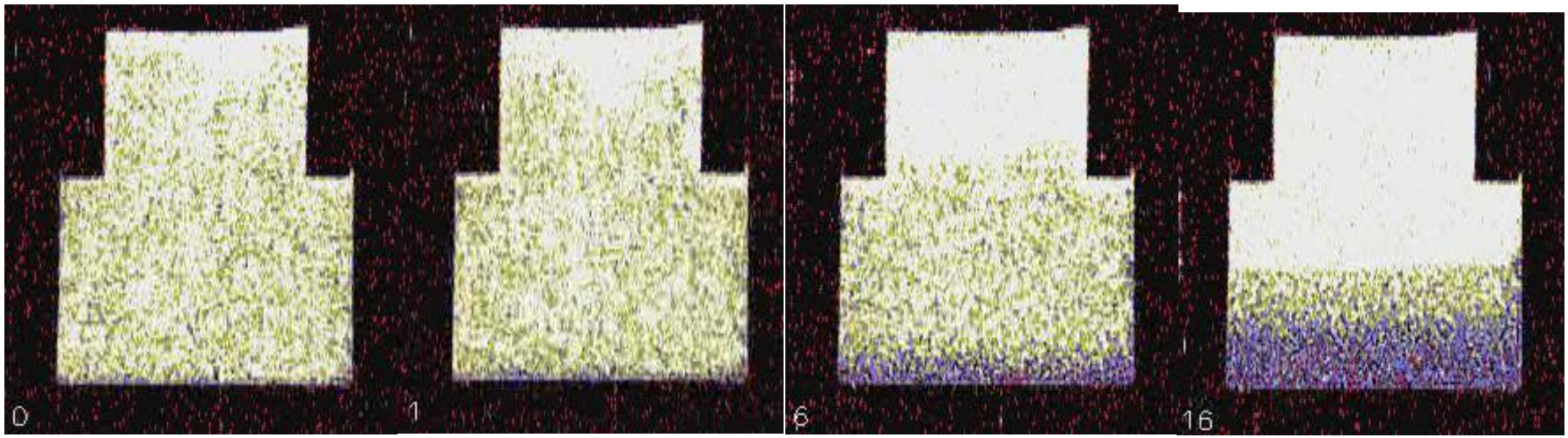

NMR imaging

Viscous Resuspension in a Rotating Couette

NMR data

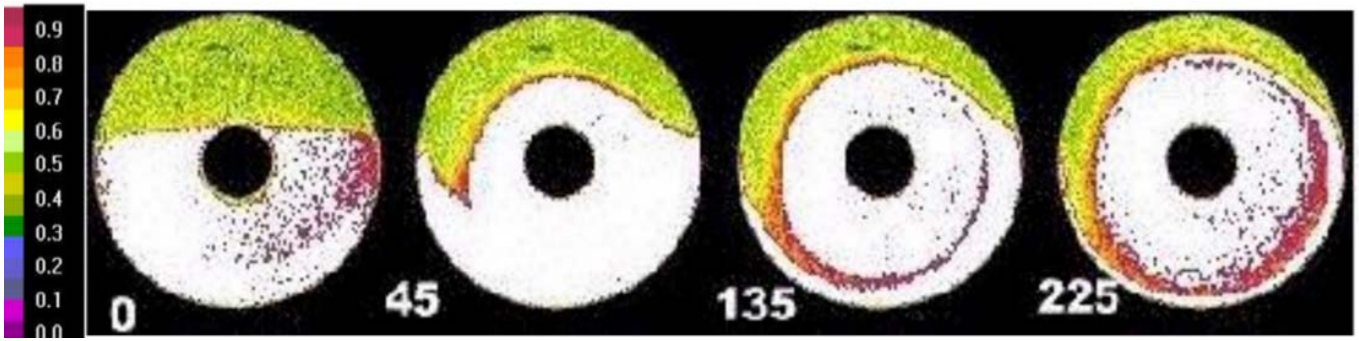

Simulation

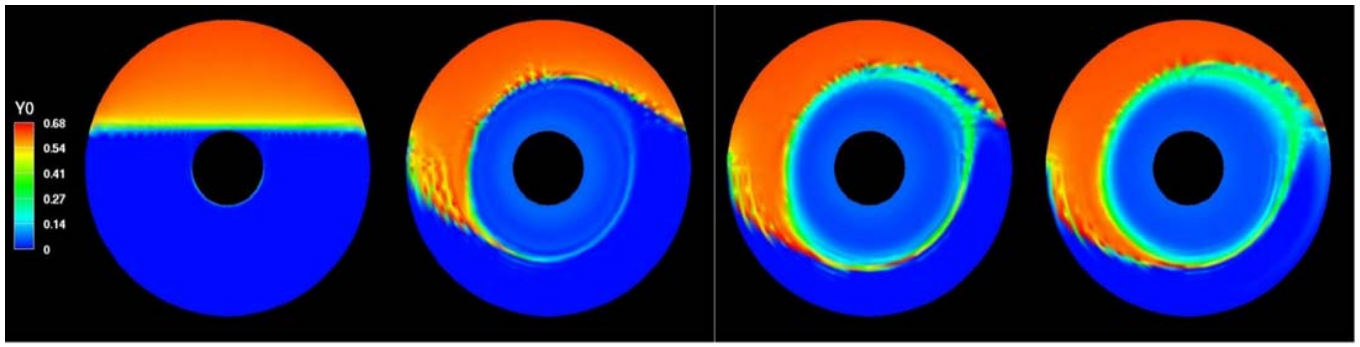

- **Once particles have floated to the top the inner cylinder is rotated at about 50 rpm**
- **Inner rod rotates and the flow "picks up" the floating particles**
- **Simulation matches experiment well for first 135 turns, then the simulation predicts somewhat slower mixing than seen in the experiment.**

Normal Stresses Important for Certain Flows: Rod Dipping in Concentrated Suspensions

From Zarraga, Hill and Leighton, J.Rheology, March 2000

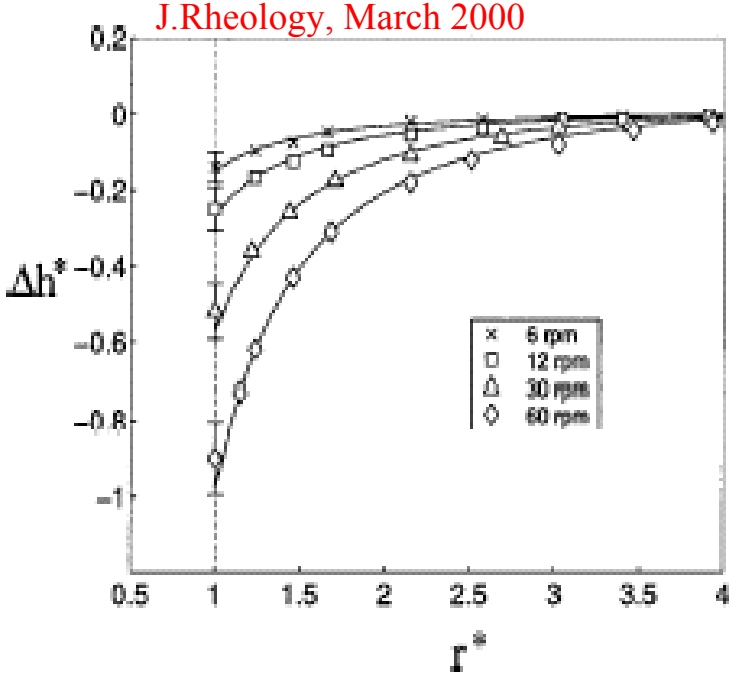

FIG. 16. Free surface profile for ϕ=0.45 (73.66 μm glass spheres in 95/5 corn syrup–glycerin mixture)

Container with inner rod rotating shows deformation of free surface for fluids with normal stresses

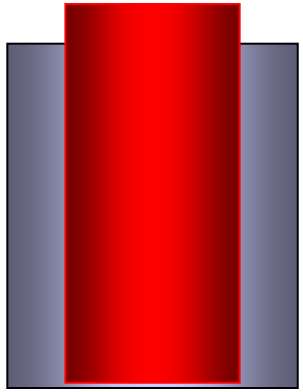

Rod climbing for polymer solutions (McKinley, MIT)

- In Newtonian solutions, rod climbing gives a relatively flat interface with a small dip due to the fluid motion interacting with the free surface
- In polymer solutions, normal forces cause fluid to climb up the rod
- In suspensions, negative normal forces create a downward dipping surface next to a rotating rod

NMR Imaging of Rod Climbing in Concentrated Suspensions

- Suspension is 50vol% 95 μm neutrally buoyant particles PMMA in Potassium Iodide/Ucon oil solution (ρ = 1.1854g/cm3, μ = 19.6 Poise)
- Wetting effects dominate profile for low rotation speeds and near the rod
- Rod dipping becomes more pronounced at higher RPMs
- Can free surface models capture the wetting dynamics and the sharp meniscus left on the rod?

NMR images for rod rotating at various rates in RPM

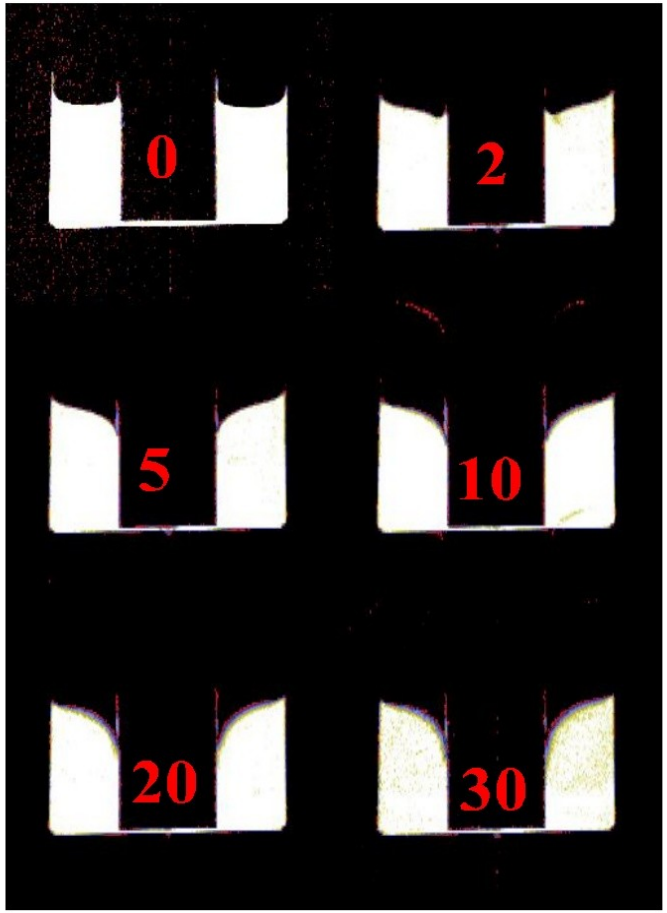

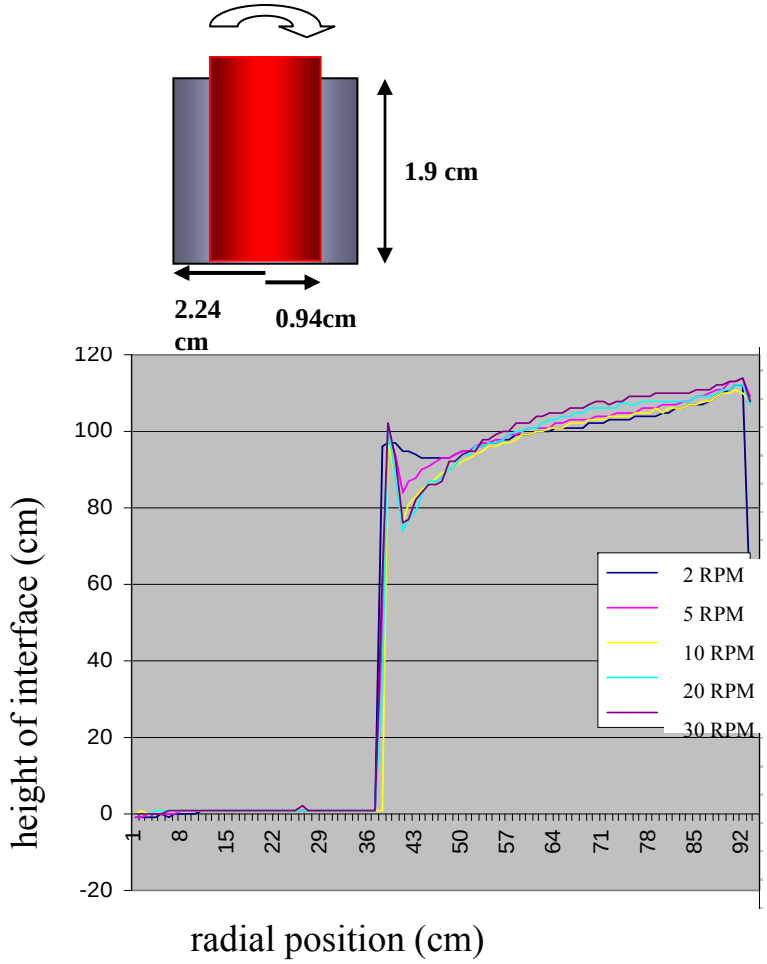

Particles show migration and a free surface that flattens with time

- Suspension is 49vol% 20/40 mesh polystyrene (850 – 425 μm) particles neutrally buoyant in Ucon lubricant
- NMR images show liquid fraction (individual pictures not scaled the same, but yellow = higher liquid content)

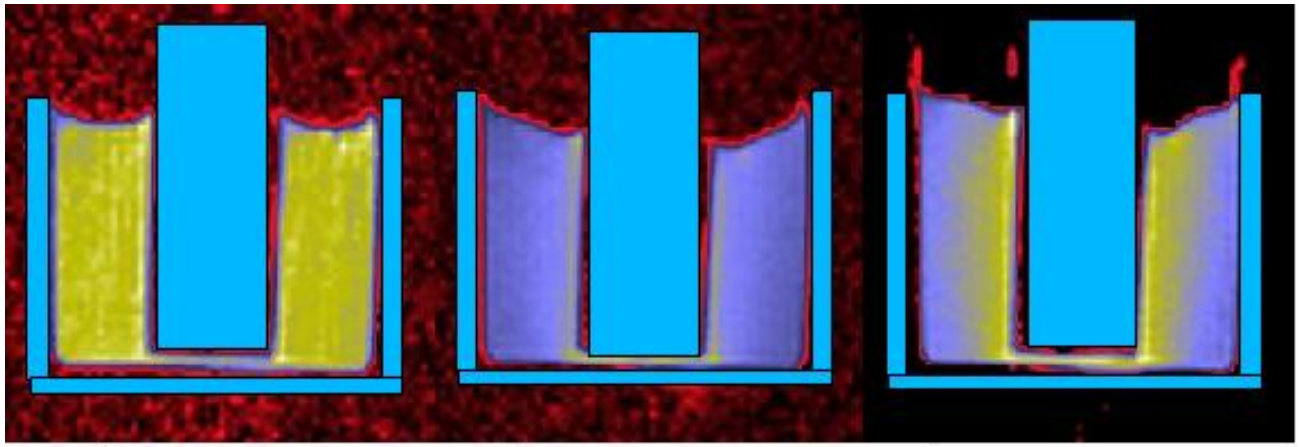

a) initial b) 20-170 turns c) 1000-1150 turns

- Can the simple diffusive flux model capture free surface shape?
- Can the diffusive flux model with the inclusion of the flow aligned tensor capture normal forces and free surface shape?

Rod Climbing in Concentrated Suspensions Modeled with Diffusive Flux Equation

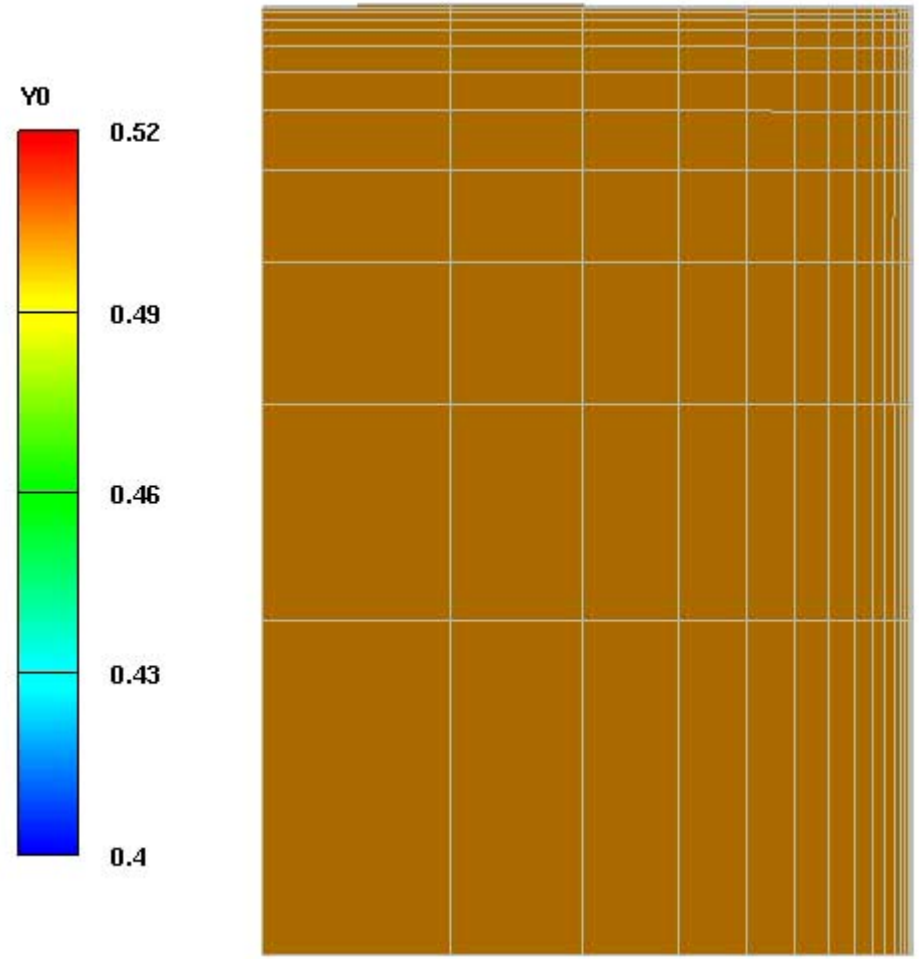

Isotropic suspension continuum models cannot capture rod dipping

Extension of Diffusive Flux Model to Include a Flow-Aligned Tensor Model (Fang et al., 2001; Hopkins et al. 2001)

Flow-Aligned Tensor Model

$$N_c = -K_c a^2 \phi \nabla \cdot (\dot{\gamma}\, \phi\, Z)$$

$$N_\eta = -K_\eta a^2 \phi^2\, \dot{\gamma}\, Z \cdot \nabla \ln \eta \quad \text{and} \quad \frac{D\rho v}{Dt} = \nabla \bullet \langle \Sigma \rangle + \rho g$$

$$\langle \Sigma \rangle = -\langle p \rangle + 2\eta(\phi)\langle \mathbf{e} \rangle - \eta(\phi)\dot{\gamma}\, \mathbf{Z}$$

The purpose of is to bias the diffusion rates along the principal flow directions (1 = flow, 2 = velocity gradient, and 3 = vorticity). Written in this coordinate system,

$$Z = \begin{pmatrix} \lambda_1 & 0 & 0 \\ 0 & \lambda_2 & 0 \\ 0 & 0 & \lambda_3 \end{pmatrix}$$

Requires that the solutions to two viscometric flows adhere to experimental results (no particle migration in torsional parallel-plate flow, and no azimuthal migration in torsional cone-and-plate flow) we find that $\lambda_1=\lambda_2$ and $\lambda_3=\lambda_1/2$.

Normal stresses arise from particle stress in momentum equation

If these directions are not known a priori, how do we compute them?

Let $\boldsymbol{u}$ = fluid velocity and $\mathbf{e} = \frac{1}{2}\left\langle \nabla \boldsymbol{v} + \nabla \boldsymbol{v}^T \right\rangle$ = rate of strain tensor.

Set $\boldsymbol{v}_{flow} = \boldsymbol{u} \big/ \| \boldsymbol{u} \|$

Solve the eigenvalue problem $\mathbf{e}\mathbf{w}_j = \zeta_j \mathbf{w}_j,\ j = 1,2,3.$

Order them such that $\zeta_1 < \zeta_2 < \zeta_3$ (for steady simple shear flows $\zeta_2 = 0$).

Set $\boldsymbol{v}_{vorticity} = \mathbf{w}_2$ (eigenvector of $\mathbf{e}$ corresponding to minimum [in absolute value] eigenvalue).

$\boldsymbol{Q = I - 1/2\ v_{vorticity} v_{vorticity}}$

Rod Climbing in Concentrated Suspensions with Q-tensor Model

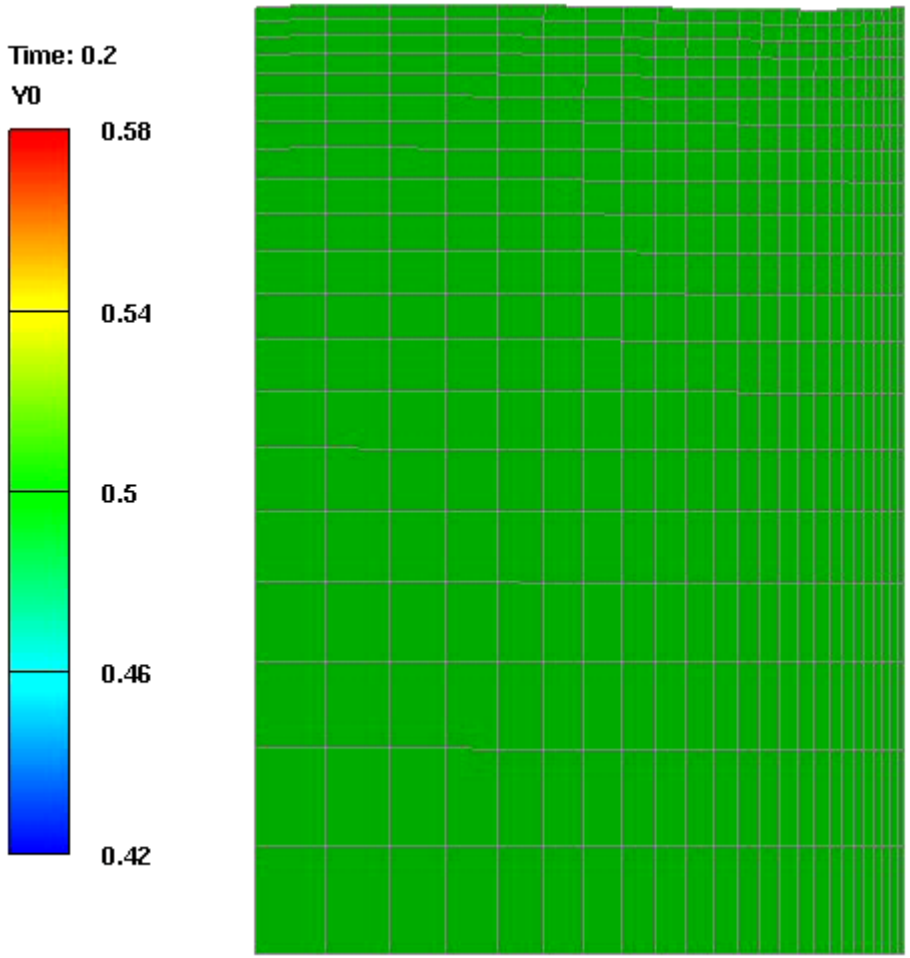

Rod Climbing in Concentrated Suspensions with Flow-Aligned Tensor in Diffusive Flux Model

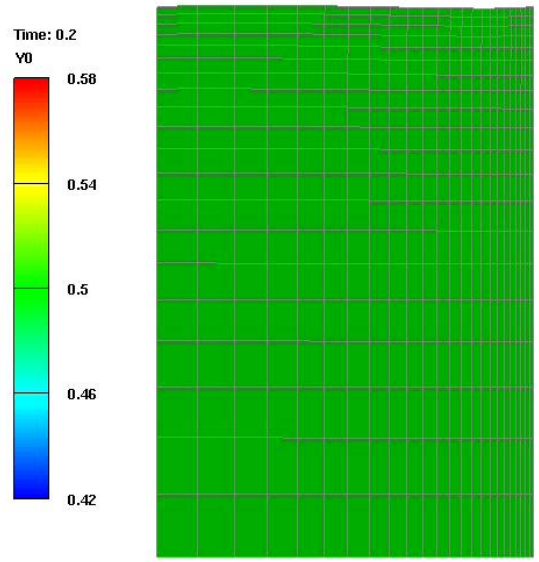

Time=0

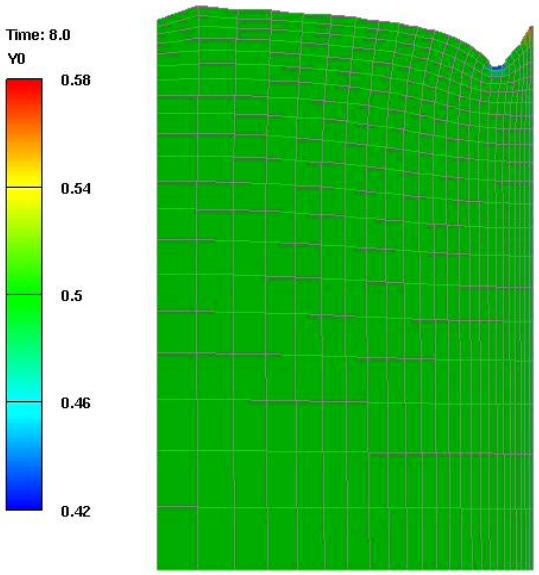

Time= 8 sec

- No mesh magnification
- Diffusive Flux model with inclusion of flow aligned tensor is used
- Rod dipping phenomena is observed
- Mesh distortion ends simulations after 8 seconds
- Cusp is very difficult to resolve with numerical methods

Free Surface Shape Evolves over Time

Model

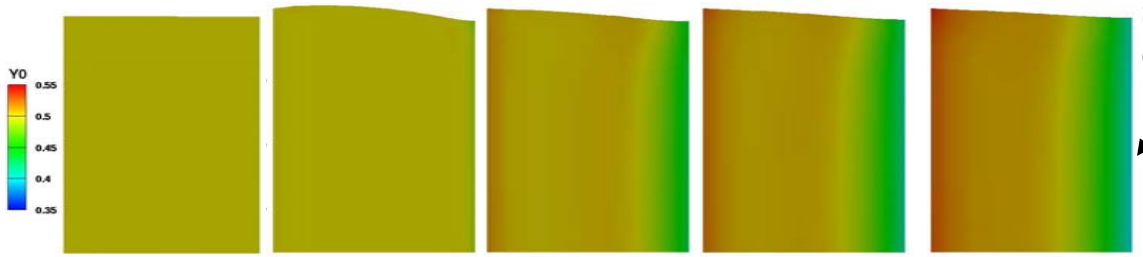

Axis of symmetry (shaft)

t = 0 t = 15s t = 510s t = 990s t = 1620s

NMR

1st picture is not on same color scale (others yellow=high liquid)

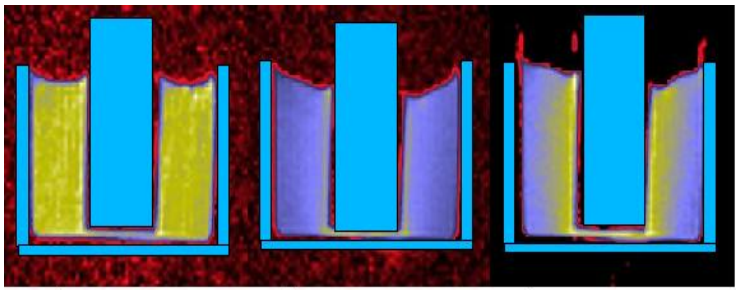

a) initial b) 20-170 turns c) 1000-1150 turns

- Elimination of wetting meniscus (slip at contact line) allows numerical simulation for longer times
- Initial condition has homogenous particle distribution and flat free surface
- After 15s, free surface shows significant “rod dipping”
- As particles migrate away from the rod, the suspension behaves more like a Newtonian fluid and less rod dipping is seen
- Particle migration seems faster for simulation than experiments

Extension of Model to Curing and Settling of Particle-Laden Epoxy

Calculations show good match to microscopy data in disk settling experiment

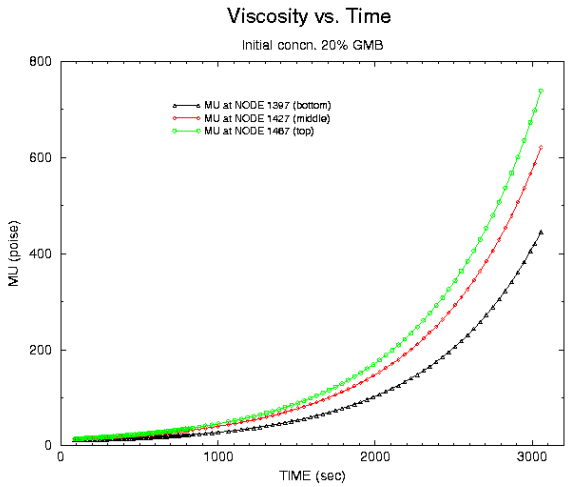

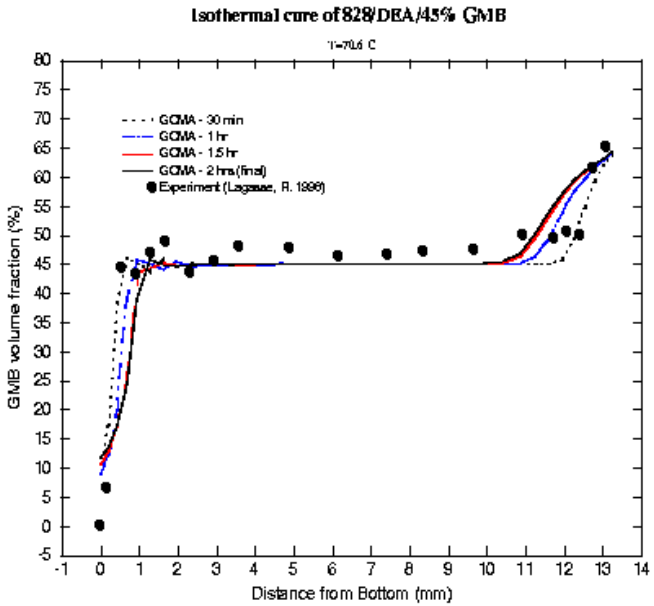

- **In addition to particle concentration, the extent of reaction, ξ, of curing epoxy impacts viscosity.**
- **Viscosity changes three orders of magnitude during curing and is sensitive to location.**
- **Initially, the material is less viscous from thermal effects. At later times, particle effects dominate the viscosity.**

$$\frac{\partial \xi}{\partial t} = \left(k_1 + k_2 \xi^m\right)(1-\xi)^n$$ **where k1, k2, and m depend on T.**

$$\eta = \eta(\phi, \xi, T) = \eta_0(T_g)\left(1 - \frac{\phi}{\phi_{\max}}\right)\left(1 - \left(\frac{\xi}{\xi_c}\right)^2\right)^{-\frac{3}{4}} 10^{-\frac{c_1(T-T_g)}{c_2+T-T_g}}$$

curing kinetics and viscosity (Adolf et al.)

disk geometry

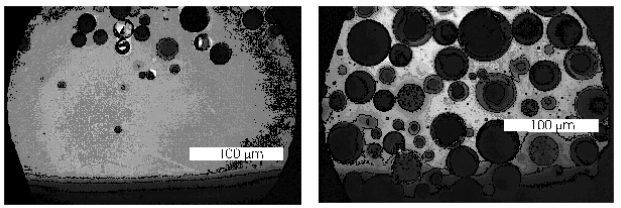

microscopy data (Lagasse)

Couette Experiment Combines Phenomena

- Mold loaded with 459 GMB using actual encapsulation process protocol (2 degassing steps)
- Shaft turned until vitrification

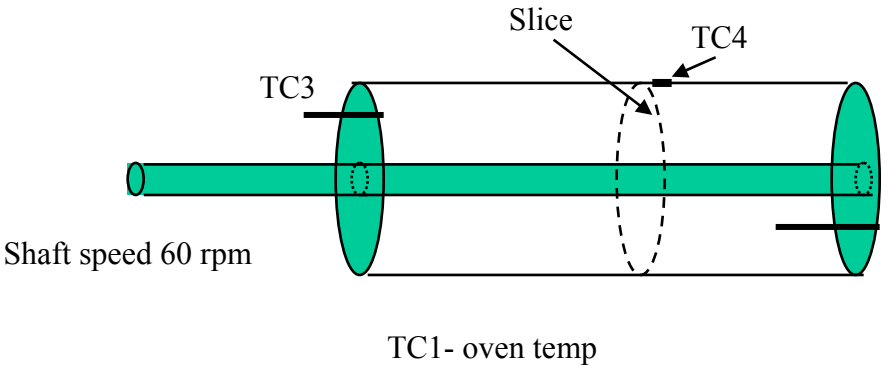

Temperature and concentration measurement locations

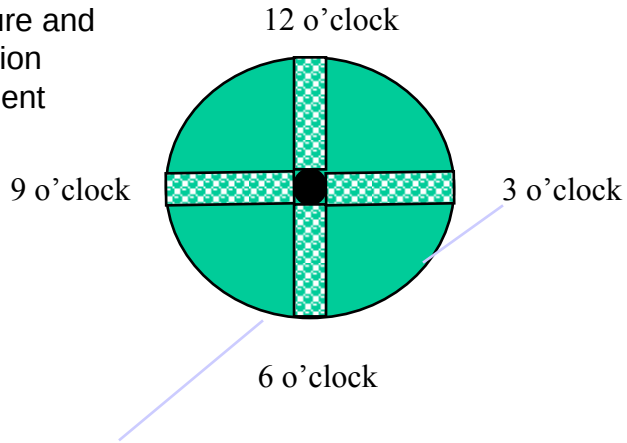

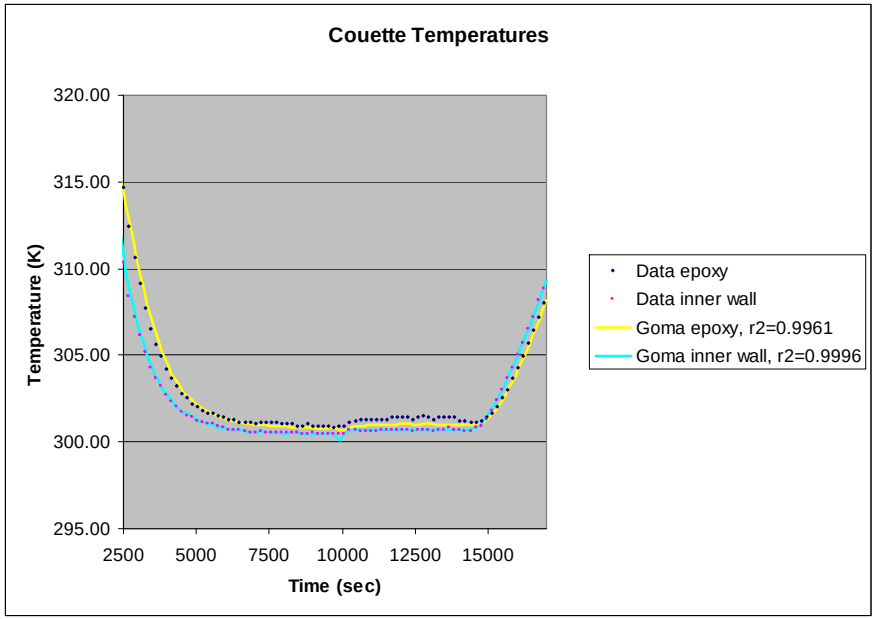

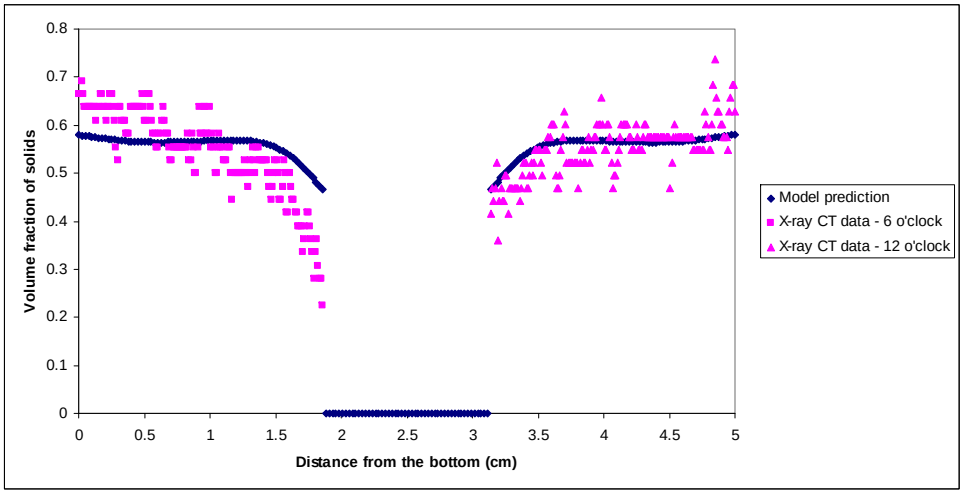

Wineglass Settling and Curing Simulations for Two Cure Schedules: Axisymmetric 2D Mesh

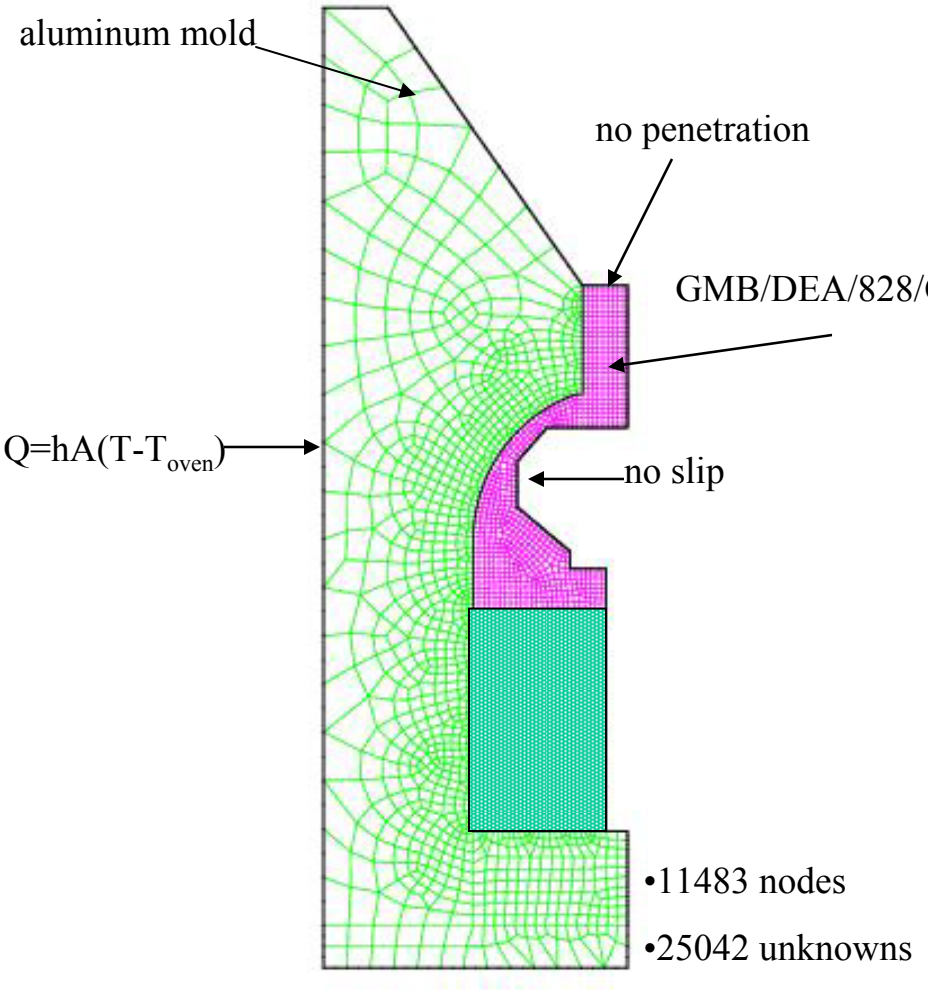

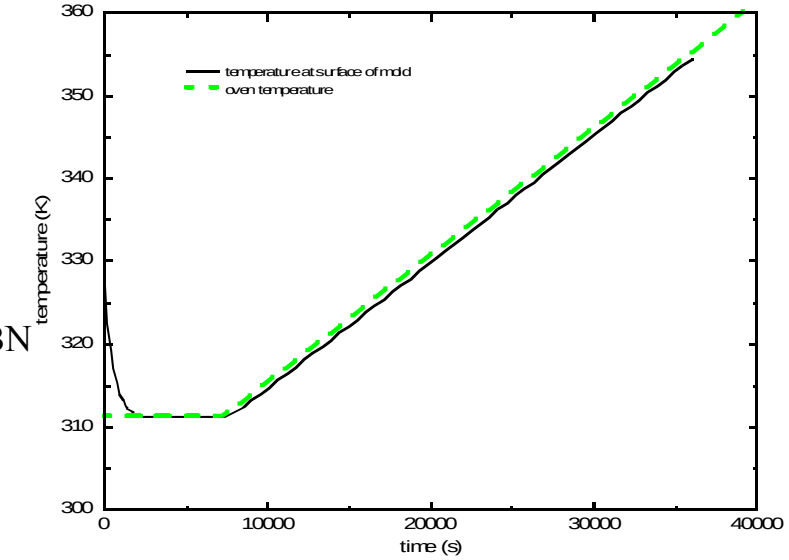

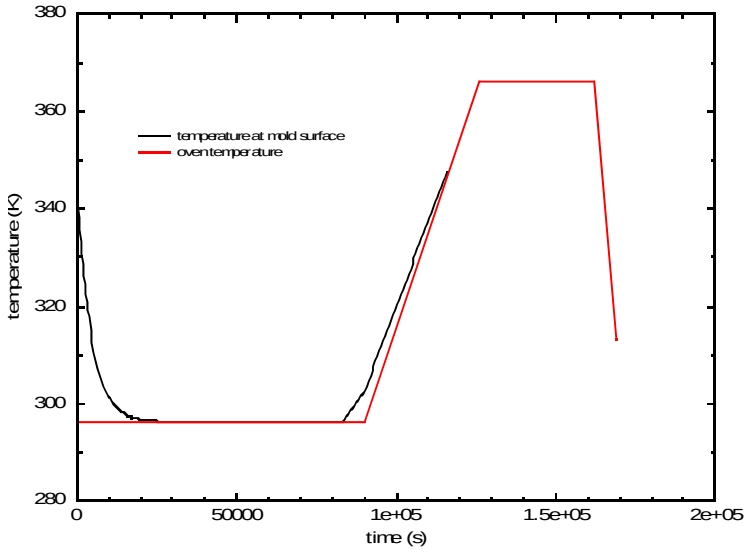

Wineglass Simulations Show Deviated Cure Schedule Produces Less Settling

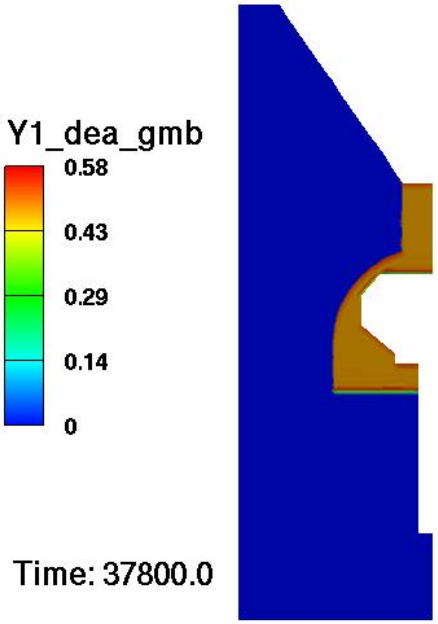

standard 24 hour cure

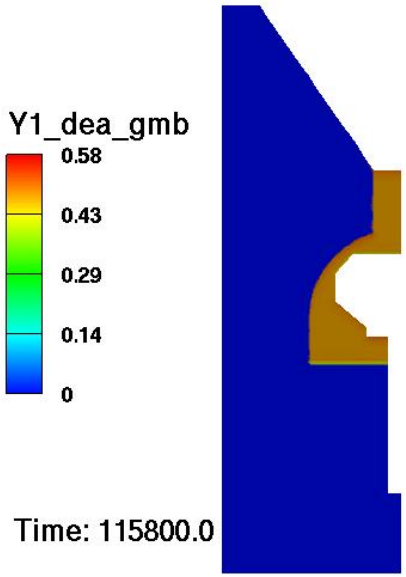

deviated 47 hour cure

- Validation data with real neutron generators should be available this FY
- Both cure schedules showed little particle settling at the gel point
- Deviated cure showed less migration for GMB
- Results were counter-intuitive due to competing phenomena: modeling is critical to determine outcome

Modeling can be used to impact real manufacturing processes

3D Curing and Settling of GMB/459 in Wineglass Geometry

A clear layer forms in an mold casting (no internal parts) Between Alox and GMB layers.

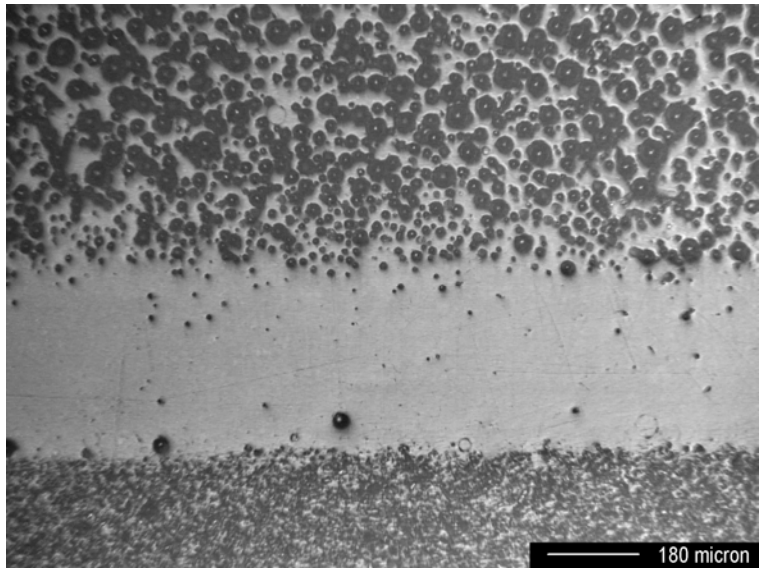

An optical micrograph shows clear layer is about 300 microns thick. *Not visible at the mold surface. (Lagasse)*

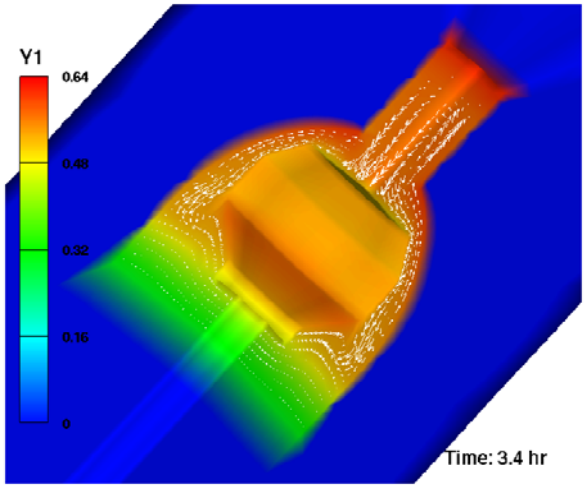

Results show significant decrease in GMB concentration at interface between suspensions

Multilayered Materials

Multilayered coextrusion combines multiple polymers in a layered structure to produce properties not found in a single polymer

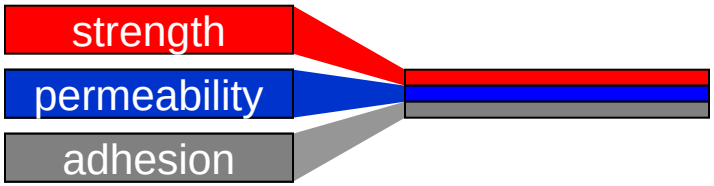

Current Applications

- Packaging (bottles, bags, etc.)
- Protection coatings
- Barrier properties

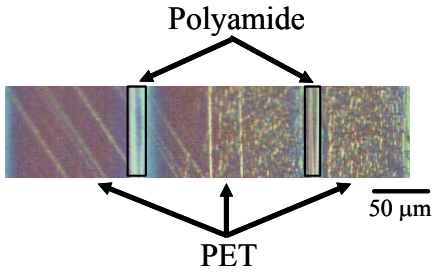

Emerging Technologies

- Energy storage devices
- Display devices
- Sensors
- Optical devices
- Barrier materials
- Membranes
- Microcomposites
- Armor applications
- Responsive clothing

Cargotech Airliner®
maintains temperature during extended transport

Multilayer Coextrusion Processing

Multiple Extruders

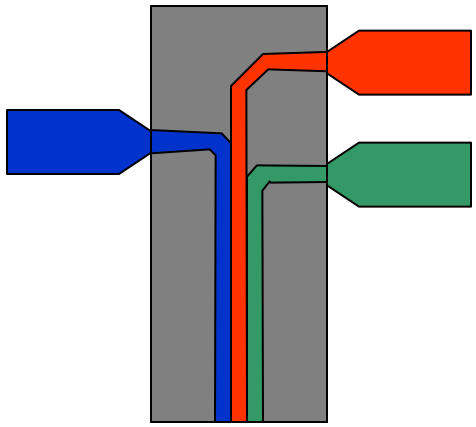

Multiplication Die

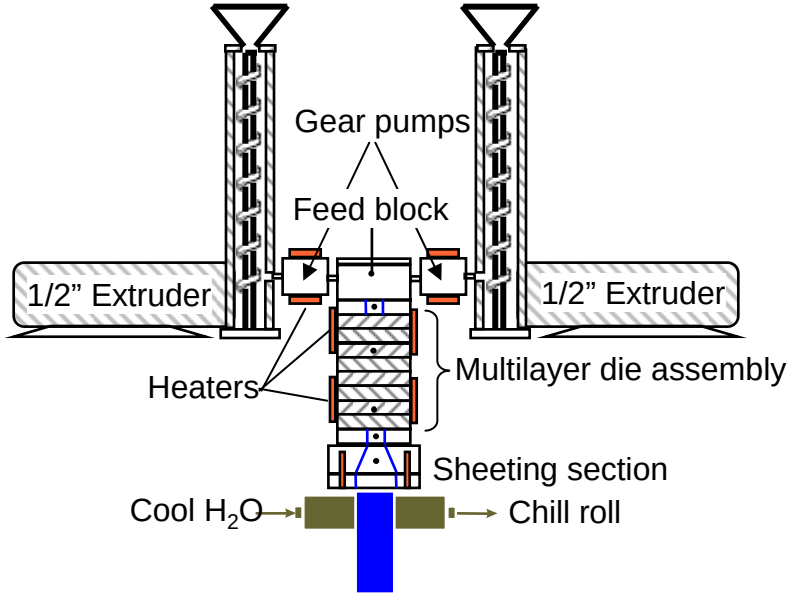

- Multilayer die assembly increases the number of layers within the same cross-section
  - Decreases layer thickness
- Gear pumps provide precise flow rate control
- Sheeting die creates ~ 1 mm tape

3M

$\delta_{PS} = 23.8 \pm 4.0\ (\mu m)$

$\delta_{PP} = 22.9 \pm 5.1\ (\mu m)$

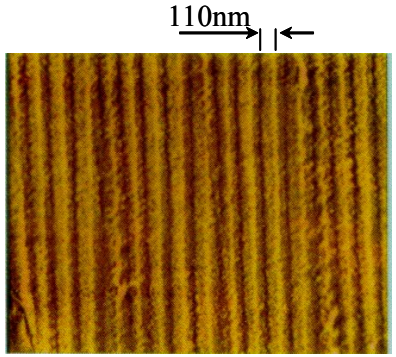

PC/PMMA multilayer, Dow Chem.

Multiplication Scheme

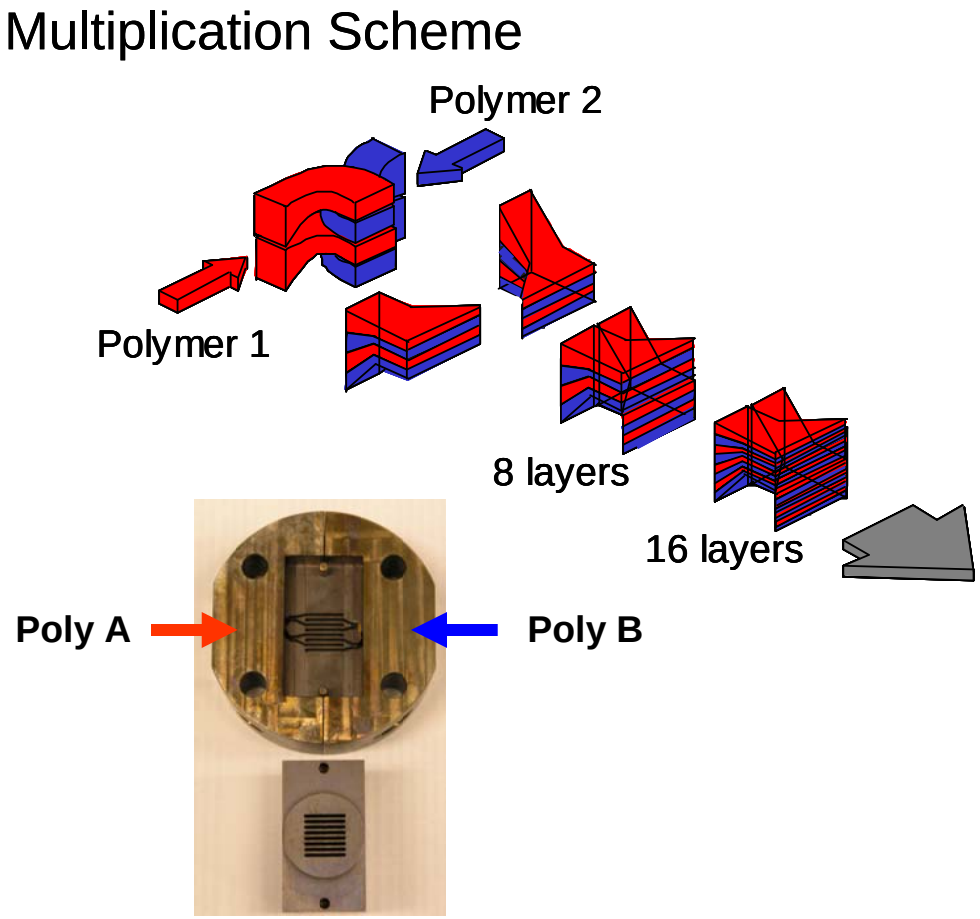

- Feedblock produces initial layered structure
- Each multiplication element doubles the number of layers
- Stacking "n" multiplication dies results in 2^{n+3} layers
- Layer stability is largely dependent on uniform laminar flow
- Thin layers (submicron) can easily break-up due to instabilities

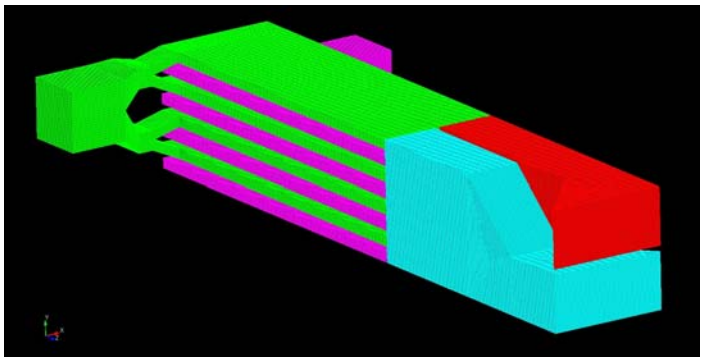

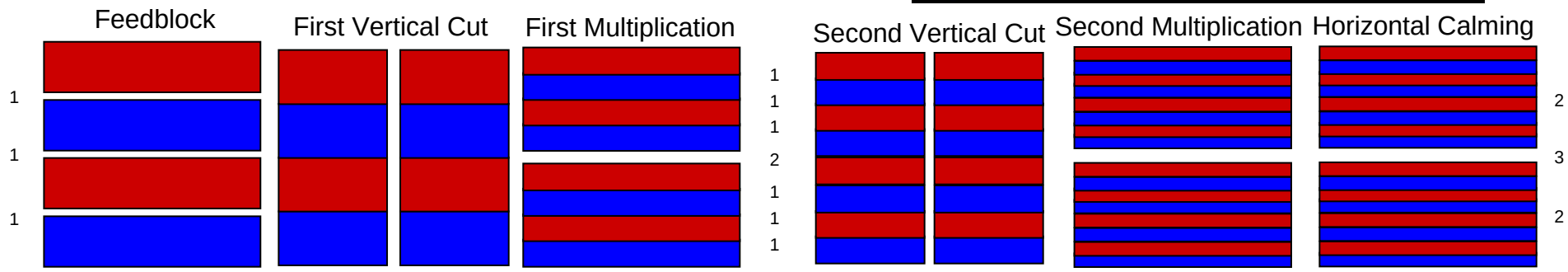

Characteristic Material Properties and Processing Parameters

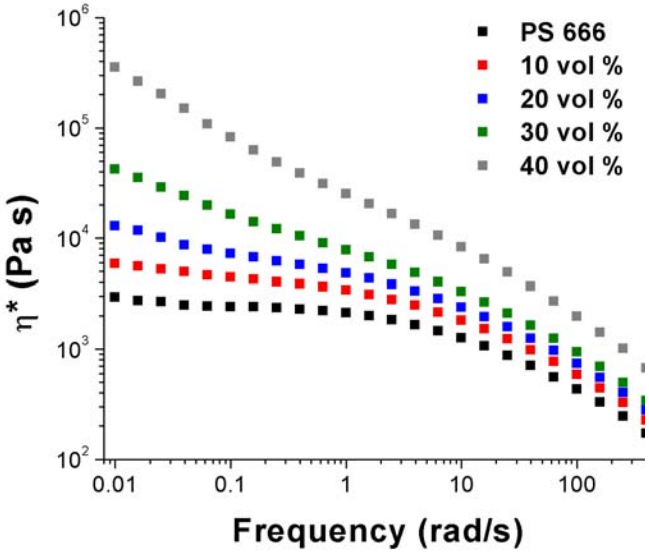

Viscosity of PS loaded with 200 nm Ni

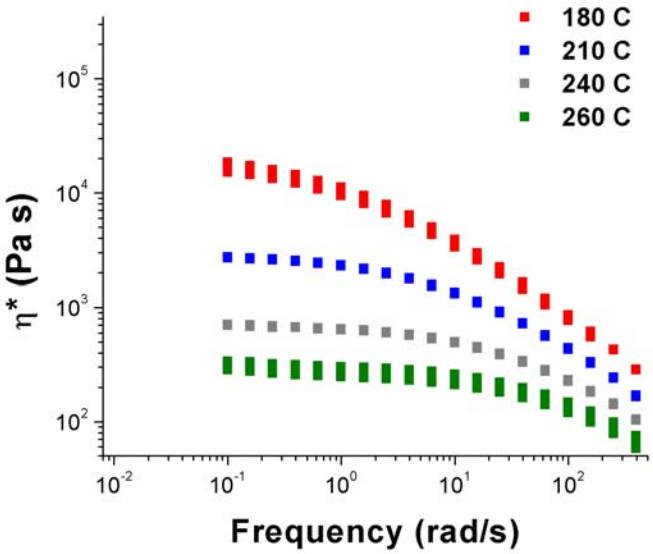

Viscosity of PS as a function of temperature

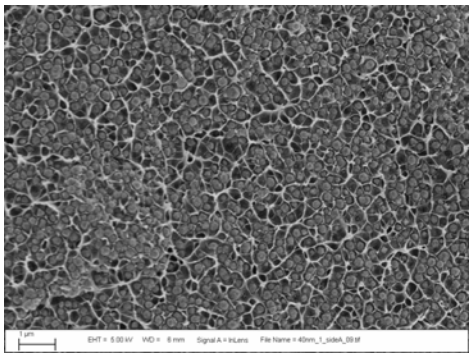

30 vol % 200 nm Ni

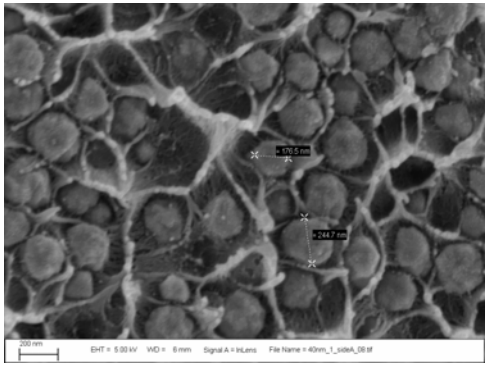

- Viscosity range 10^3-10^5 Pa s
- Density range 1-5 g/cm^3
- Velocities 0.25-4 cm/s
- Interfacial tension, ?

Questions We Want to Answer Using Modeling

- Can we directly create an offset die that produces an encapsulated red phase?
  - •3D modeling could answer this question
- What happens to the flow in the splitter?
  - •3D modeling gives layer thickness after the splitter
- How do we produce stable films (ribbing, barring, rivulets, encapsulation, etc.)
  - •What viscosity ratios will be stable?
  - •For filled systems, what density ratios will be stable?
    - •Linear stability analysis
- Effects of rheology? Operating window? (Maybe next year …)

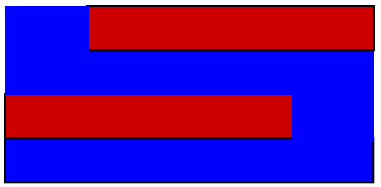

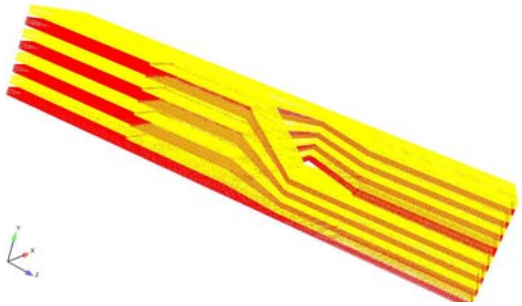

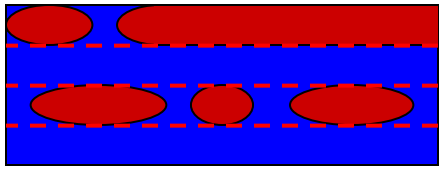

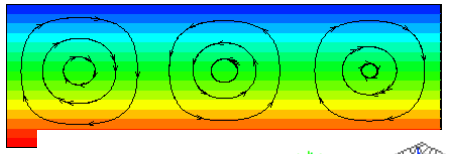

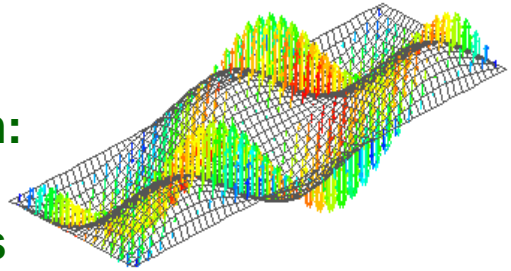

Methods developed for coating flows used for coextrusion: Coating consortium at Sandia (CRMPC) driver for computational analysis tools for manufacturing processes

3D Mesh of Two-Layer Coextrusion Multiplication Region to Four-Layer Structure

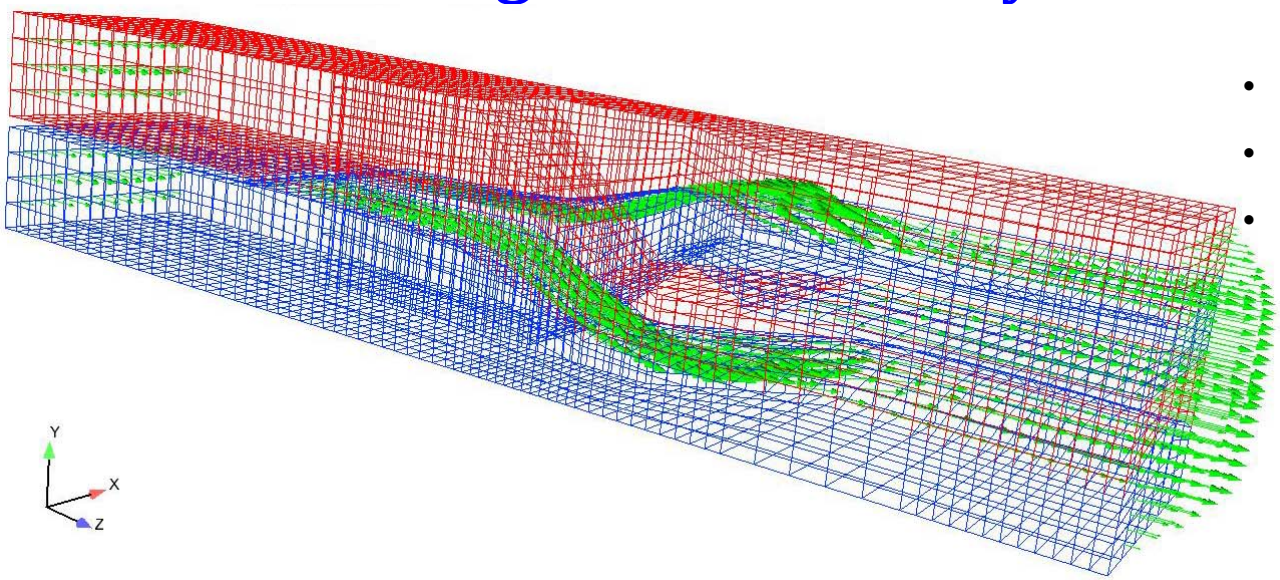

- 9276 8-Node hexahedral elements
- 12040 Nodes
- 84280 total degrees of freedom

- Flow splitters and duct wall all have no slip boundary conditions
- Free surface exists between red and blue fluid in the downstream region, where surface tension and kinematic condition are applied
- Inflow boundaries have constant applied pressure
- Boundary conditions must be applied to momentum equations and mesh equations
- Sixteen different side sets in the mesh

Fluid 1: Top fluid

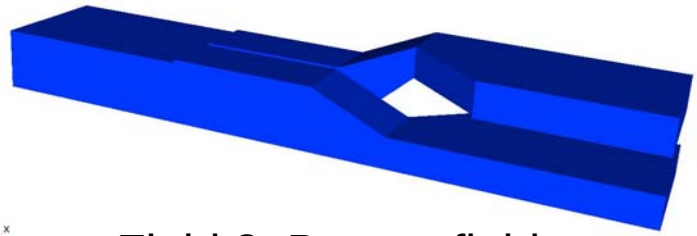

Fluid 2: Bottom fluid

Effect of Viscosity Mismatch? Continuation in Red Fluid Viscosity

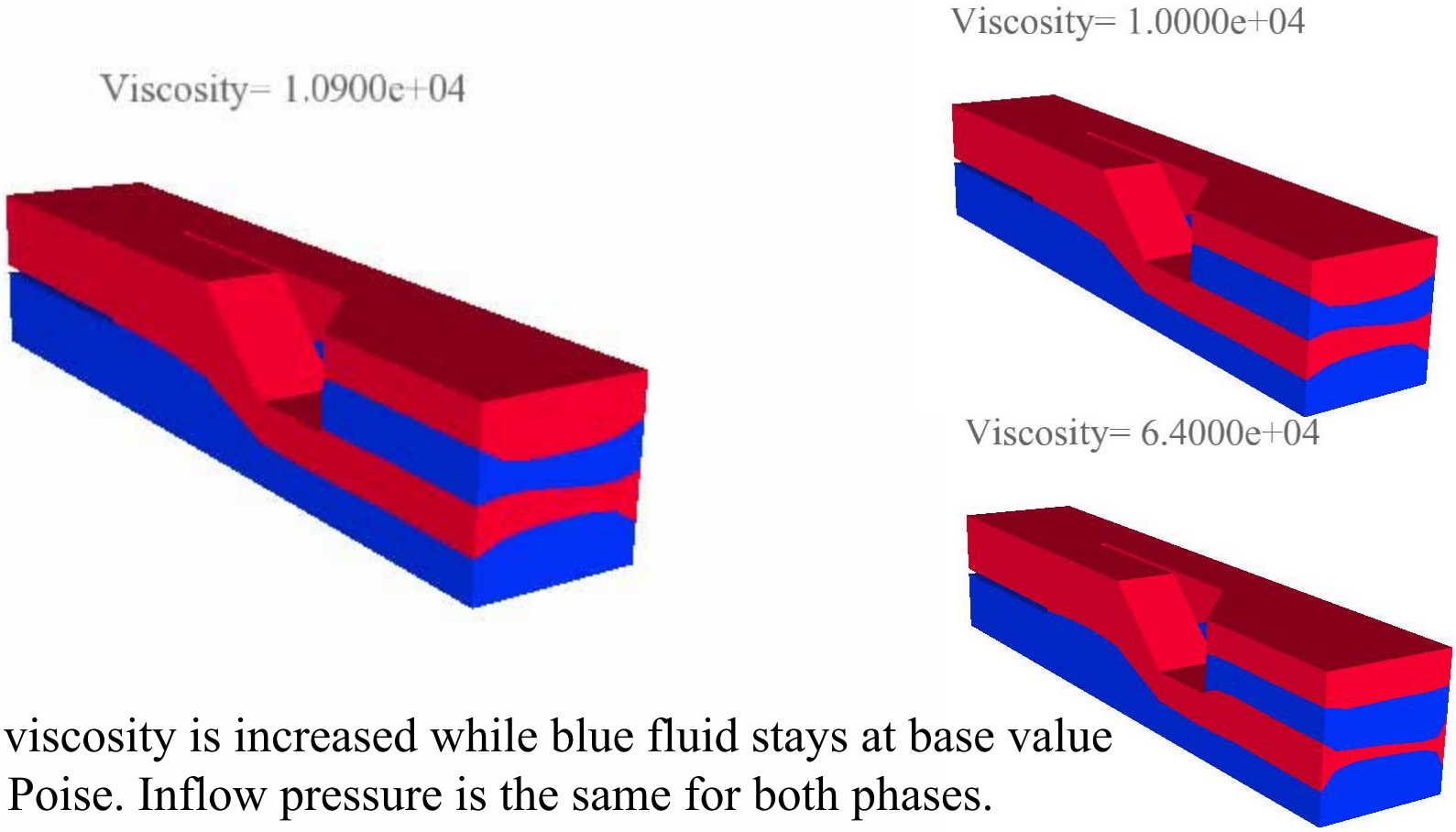

- Red fluid viscosity is increased while blue fluid stays at base value of 10,000 Poise. Inflow pressure is the same for both phases.
- Blue fluid squeezes out red fluid until the bottom red layer is nearly gone
- Simulations discontinued as mesh becomes too deformed
- 3D deformed geometry remeshing would be helpful
- Boundary conditions could be relaxed from no slip

Effect of Pressure Mismatch?
Continuation in Red Fluid Inflow Pressure

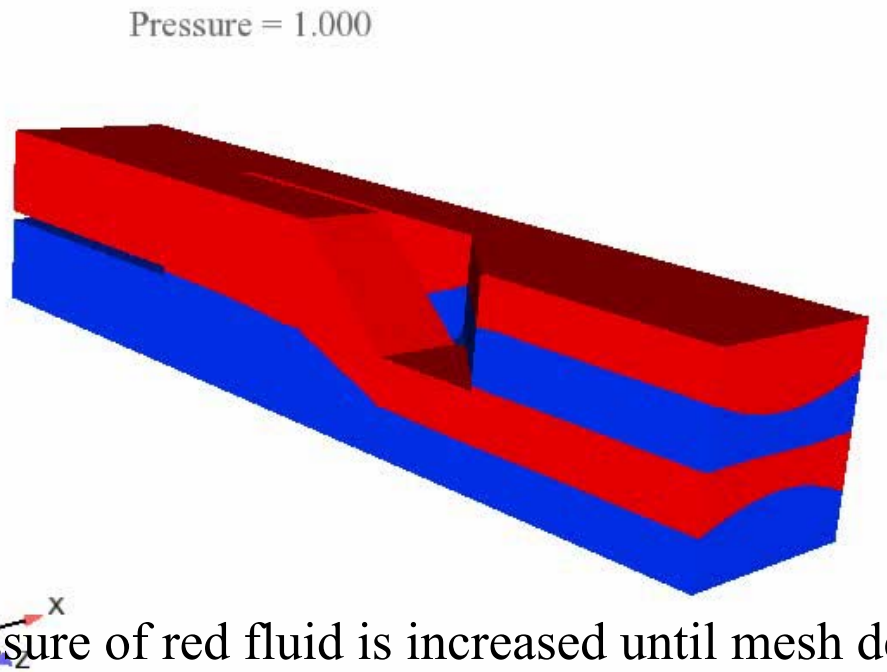

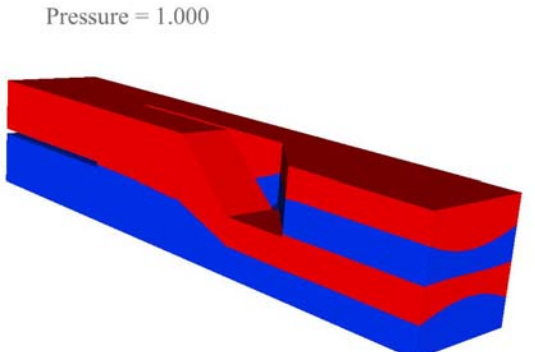

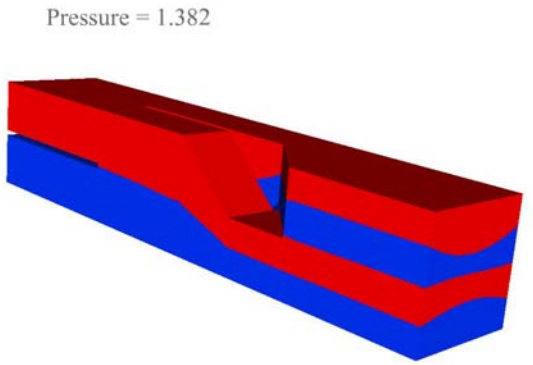

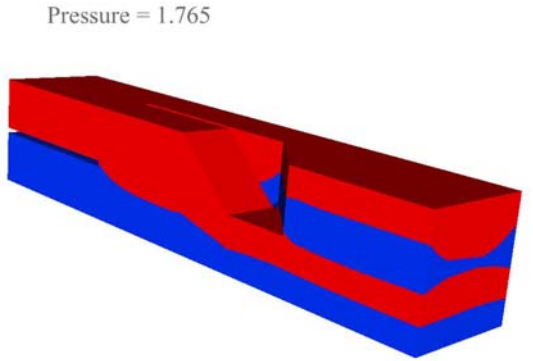

- Pressure of red fluid is increased until mesh deformation become too great
- Both and blue fluid viscosity are 10,000 Poise
- Red fluid squeezes out blue fluid until the top blue layer is nearly gone
- Nondimensionalization improved solver performance, reducing average iterations from 180 to 30

Can We Use From Fixed Mesh Solution Particle Tracking To Determine Layer Thicknesses?

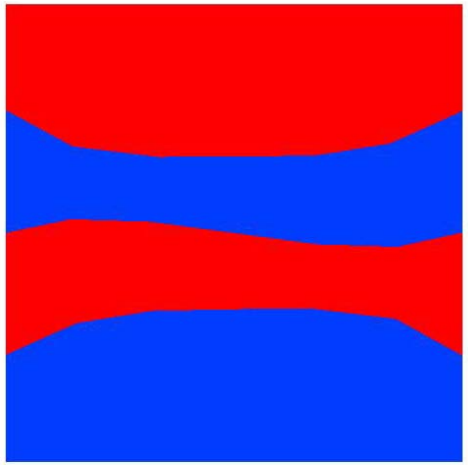

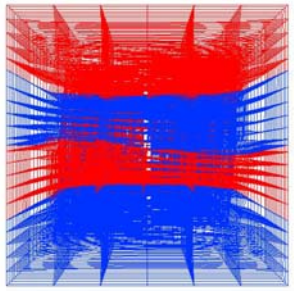

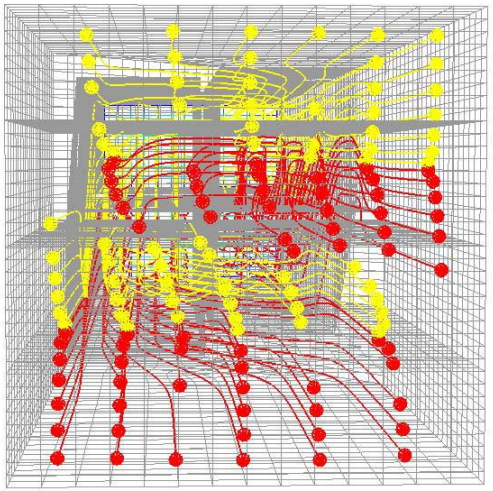

Solution for equal properties and flow rates using kinematic condition between layers

Particle traces indicate flow and layer thickness from fixed mesh solution for equal properties and flow rate

- Particle tracking from the inflow from the fix mesh solution predicts layer thickness and shape different from moving mesh solution
- Lack of kinematic condition could be the reason for the dissimilar results

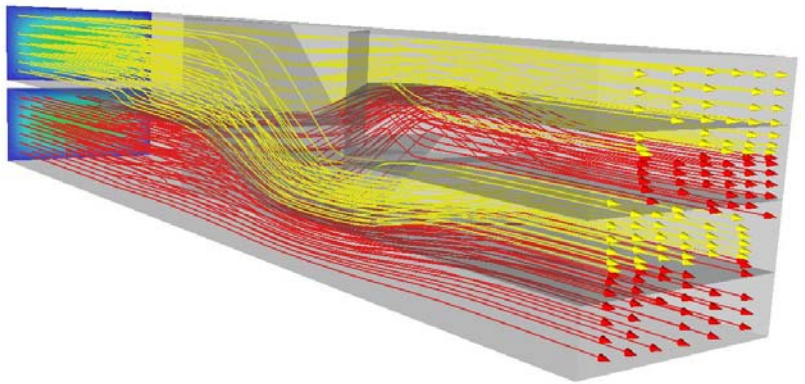

Comparison of ALE and Level-Set Coextrusion Simulations

ALE simulation

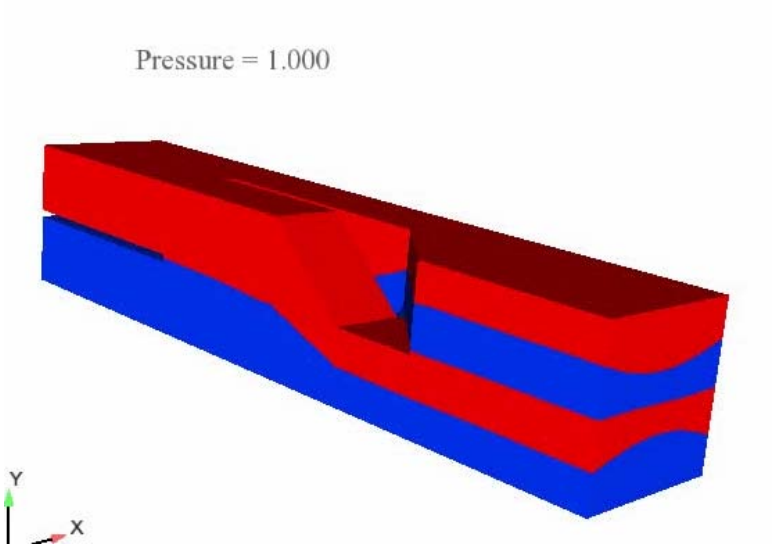

Level-set simulation

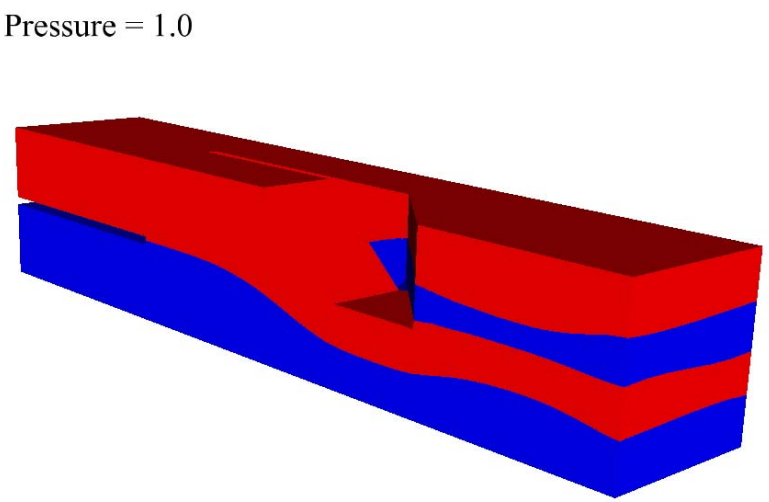

- In both simulations, the fluid viscosities are each 10000 Poise
- Blue fluid squeezes out red fluid until the bottom red layer is nearly gone
- Differences are due to boundary conditions along the walls contacting the free surface – ALE simulations use a no-slip condition, while level-set simulations use a Navier-slip condition on these walls

Comparison of ALE and Level-Set Coextrusion Simulations

ALE simulation

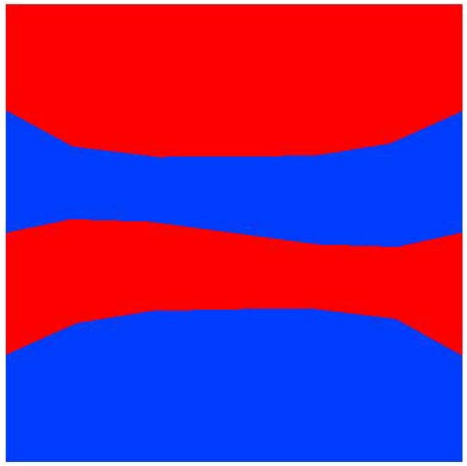

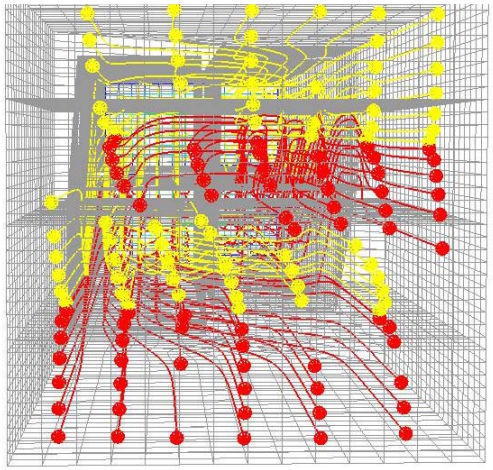

Level-set simulation

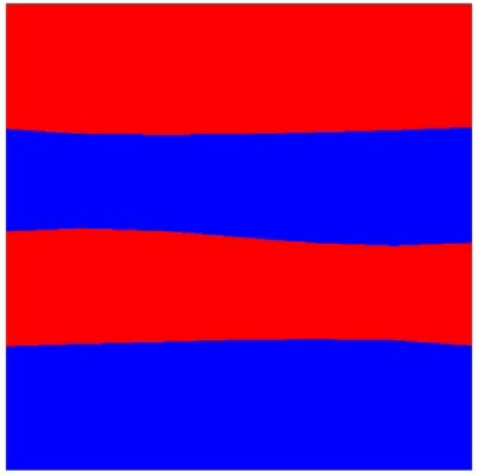

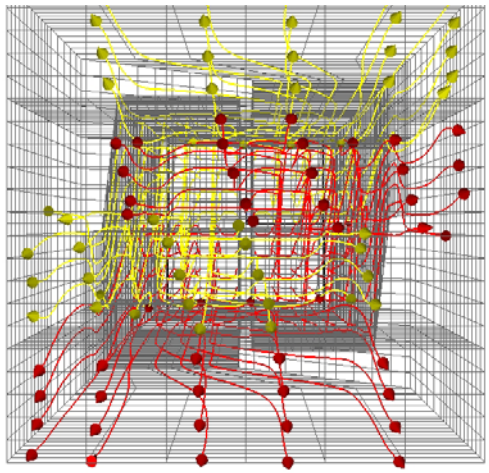

Simulation of Two-layer Coextrusion with Level-set Interface Tracking

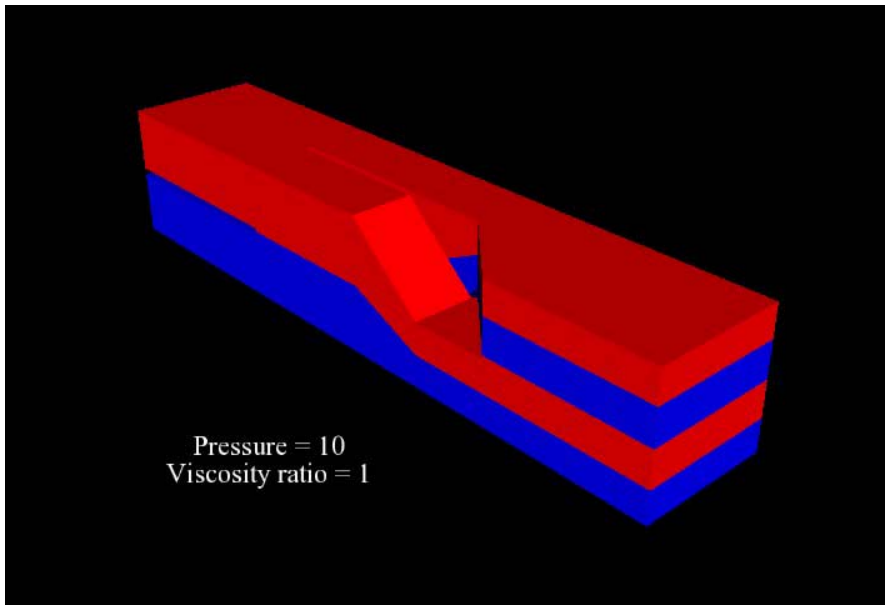

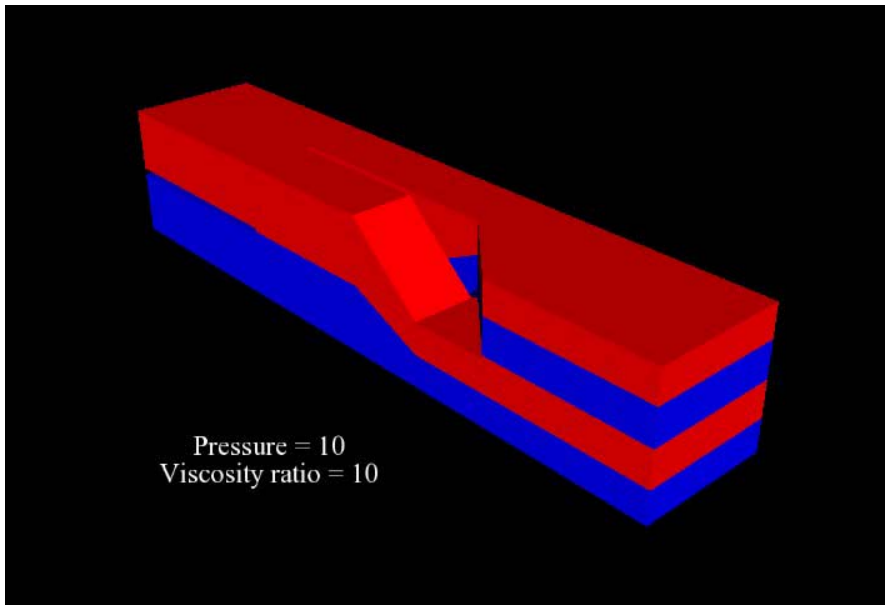

- Time-dependent simulations of two-layer coextrusion using level-set interface tracking
- Blue fluid squeezes out red fluid, thinning the bottom red layer
- At high viscosity ratios, the more viscous (blue) fluid layers merge in part of the channel, destroying the integrity of the lamellae

Simulation of Two-layer Coextrusion with Level-set Interface Tracking

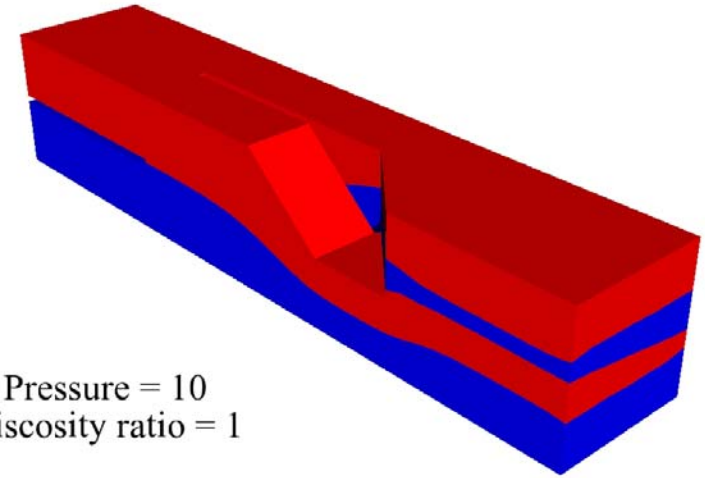

Pressure = 10
Viscosity ratio = 1

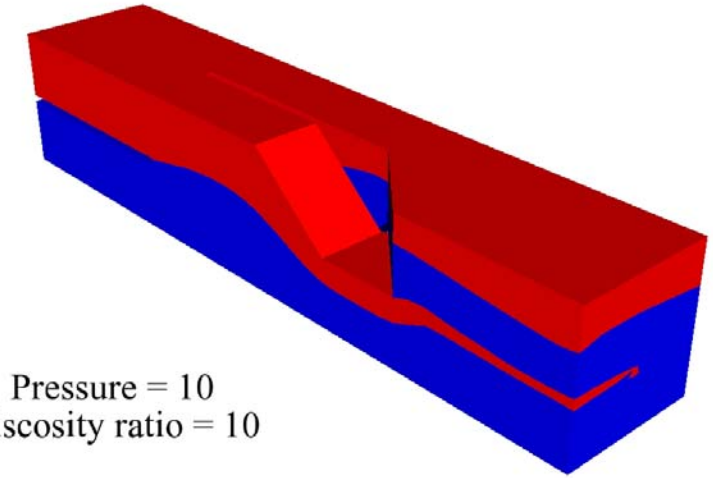

Pressure = 10
Viscosity ratio = 10

- Time-dependent simulations of two-layer coextrusion using level-set interface tracking
- Blue fluid squeezes out red fluid, thinning the bottom red layer
- At high viscosity ratios, the more viscous (blue) fluid layers merge in part of the channel, destroying the integrity of the lamellae

Thixotropic Model with Structure Factor to Capture Agglomeration/Breakup and Time-Dependence

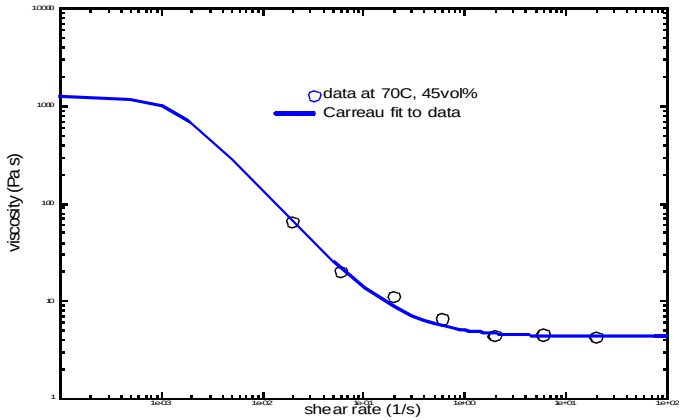

Steady State Viscosity Data of Alox suspension at 70°C (symbols) fit to a Carreau-Yasuda Model (line)

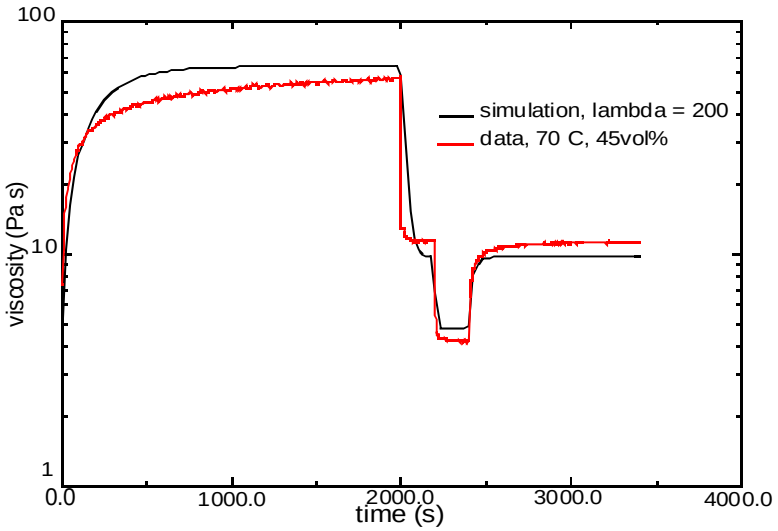

- Initial model includes aggregation network
  - Model by Adolf, inspired by ideas in Mujumdar, Beris, & Metzner (JNNFM 2002)
  - Captures time-dependent response and steady-state viscosity
  - Currently ignores polymerization, particle migration and particle settling

$$\frac{d\xi}{dt} = -k_r\,\dot{\gamma}^{m}\,\xi + k_f(1-\xi)$$

$$k_r = k_r^o e^{-\frac{E_b}{RT}}$$

$$\xi = \frac{[b]}{[b_{\max}]}$$

$$k_f = k_f^o e^{-\frac{E_f}{RT}}$$

$$\eta = \eta_\infty + (\eta_o - \eta_\infty)\xi^p$$

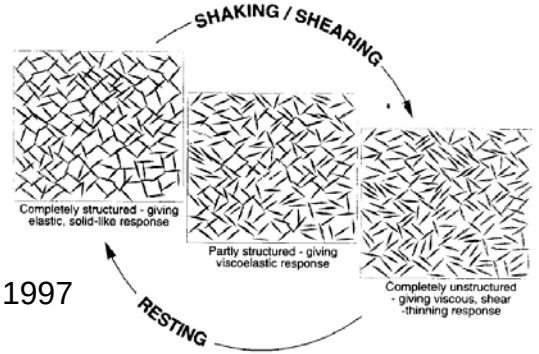

Barnes 1997

Goal: To Use Numerical Modeling To Help Optimize The Injection Process

- Finite element models of injection process
  - –Complex free surface flow
  - – Constitutive equation description
  - – Nonisothermal flow
  - – 3D geometry

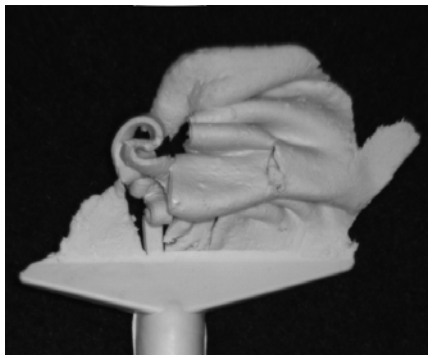

2.5 mm shot, 40% injection speed

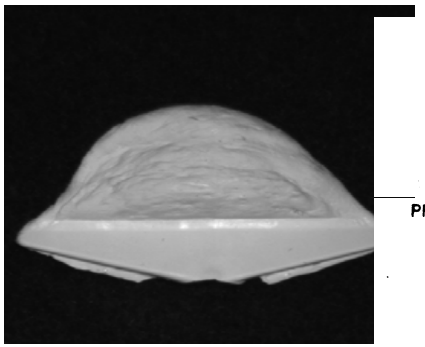

2.5 mm shot, 100% injection speed

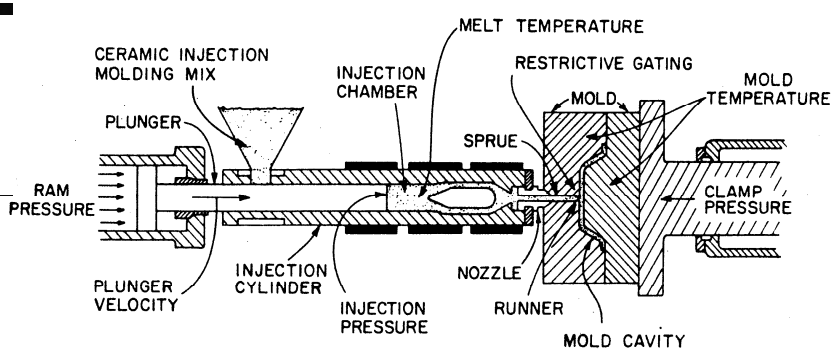

Short shots show that incomplete filling can occur for poorly optimized process parameters

Carreau-Yasuda Model Includes Shear-Thinning and Temperature Dependence

- Temperature dependent viscosity data determined from a capillary rheometer
- Raw data corrected with Rabinowitsch correction for slip
- Non-linear least-squares Gauss-Newton method to estimate D, l, a, and n (requires initial guess of parameters to be estimated) with fixed μ_0 and μ_∞

$$\mu = a_T\left[\mu_\infty + (\mu_0 - \mu_\infty)(1 + (a_T\lambda\dot{\gamma})^a)^{\frac{(n-1)}{a}}\right]$$

where $a_T = e^{D/T}$

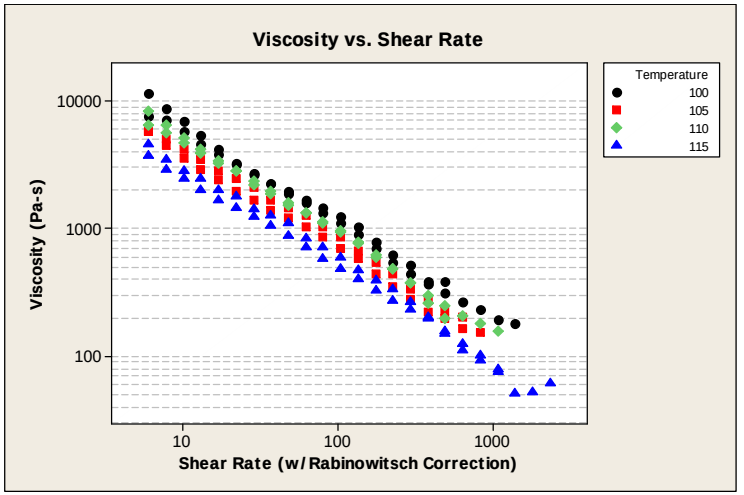

μ_0	μ_∞	n	a	λ	D	Mean	Std Dev
2,000	30	0.2	6.28	0.8	100	-4.93	14.65
2,000	32	0.2	6.2	0.8	100	-7.4	14.61
2,000	35	0.2	6.06	0.8	100	-11.1	14.55

Mean closest to zero and lowest standard deviation of residuals indicate better fit.

FEM Mesh and Boundary Conditions for 2D Mold Filling

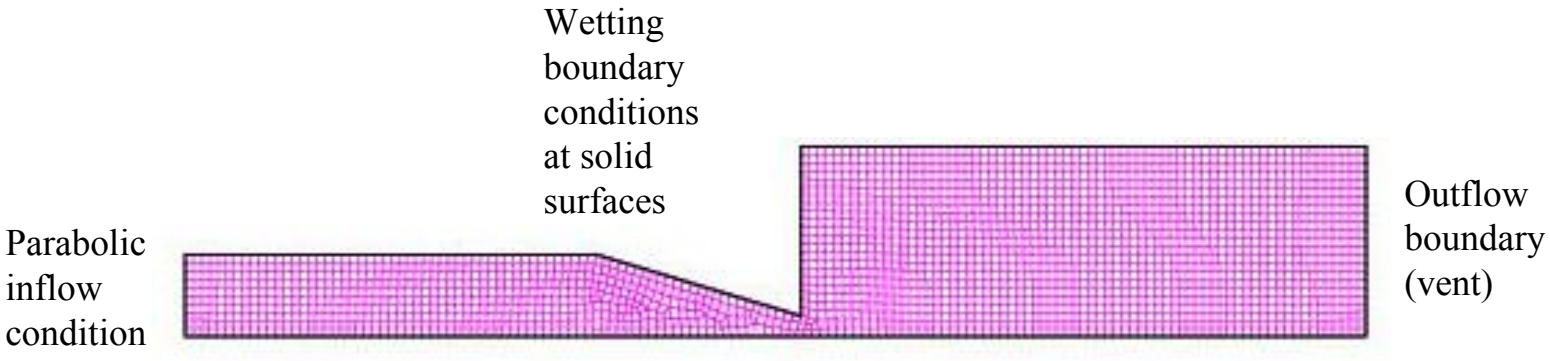

- Biquadratic velocity/ Bilinear pressure interpolation
- LBB element
- Direct solution of fully coupled matrix
- 2244 9-Node 2D quadrilateral elements
- 9321 nodes, 30380 total degrees of freedom

Comparison of Newtonian and Highly Shear-Thinning Carreau Models for 2D Mold Filling

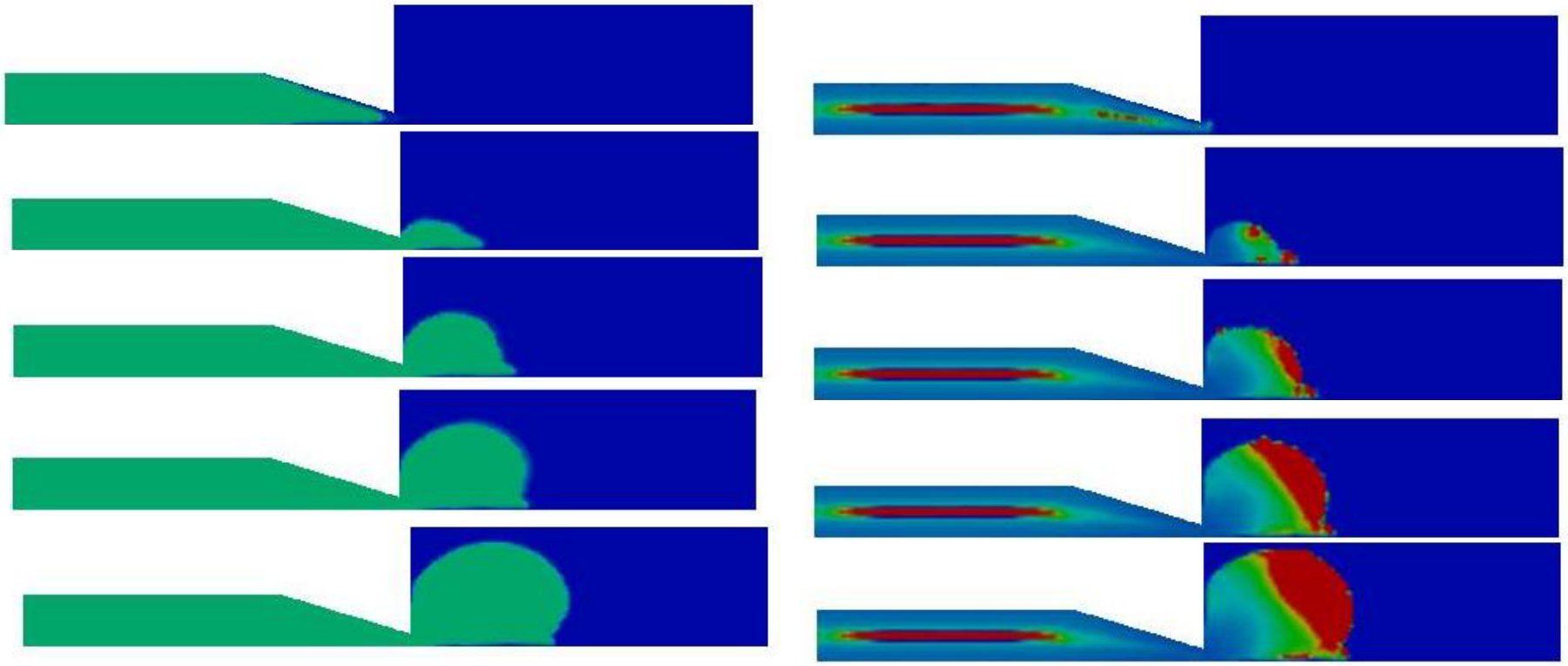

- Wetting physics dominate shape of interface
- Shear-thinning fluids fill slightly faster than Newtonian
- Shear-thinning viscosity ranges from 20,000 to 300 poise

Injection Molding of Ceramic Pastes

- Suspensions are multiphase materials that have very complex flow behavior
- Current material models for particle suspensions predict effect of:
  - Temperature
  - Flow rate
  - Time/history
  - Particle size and concentration
- Our modeling has predicted in non-isothermal injection molding of ceramic precursor pastes

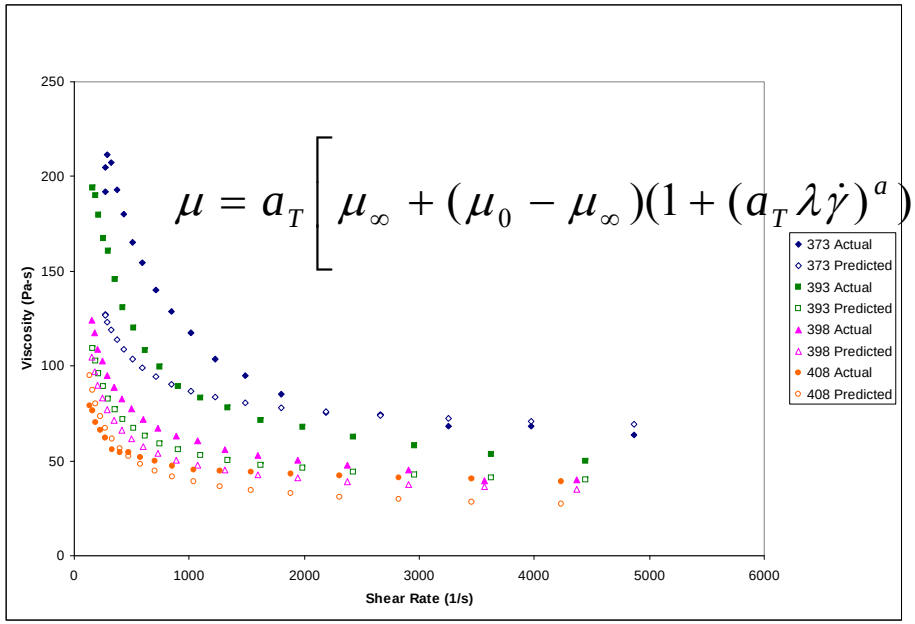

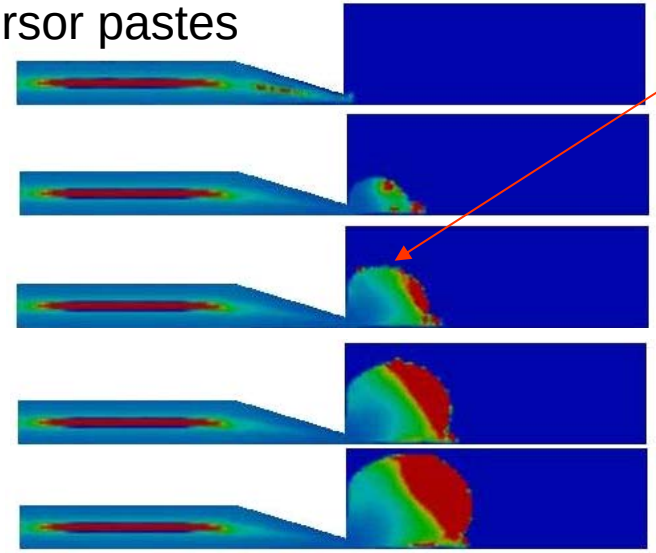

flow front

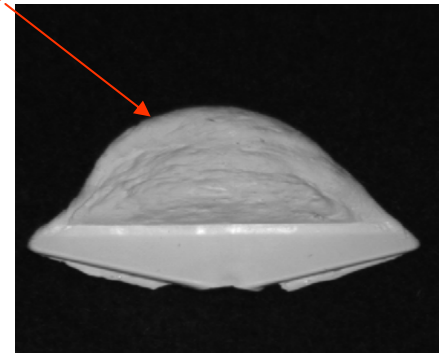

Temperature-dependent rheology and fit to a Carreau-Yasuda model (L. Mondy and L. Halbleib)

Model was validated with experiments in which partially filled mold was quickly cooled to capture intermediate state (R. Rao, P. Yang)

Blake Wetting Line Model

- Molecular Kinetic Model

T.J. Blake, J. De Coninck *Adv. Colloid Int. Sci.* **2002**, *96*, 21-36.

Adhesion to Substrate

$$U = \frac{2kT\lambda}{\eta v_L}\exp\left[\frac{-\gamma_{LV}(1+\cos\theta_\infty)}{nkT}\right]\sinh\left[\frac{\gamma_{LV}(\cos\theta_\infty-\cos\theta)}{2nkT}\right]$$

Viscosity

Molecular-Kinetic

Lump terms

$$U = v_o \sinh\left[\gamma(\cos\theta_\infty-\cos\theta)\right]$$

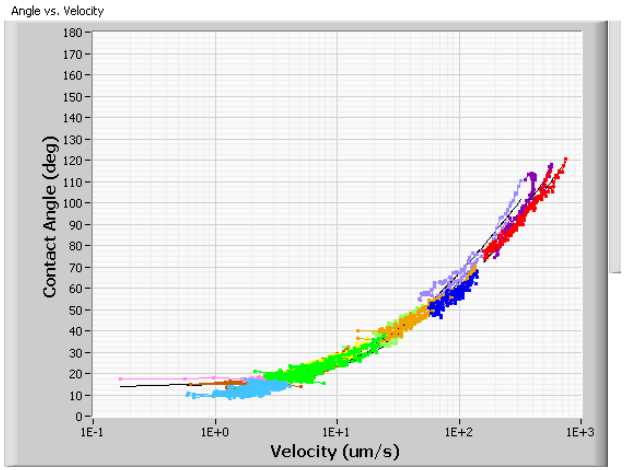

Goniometer wetting data

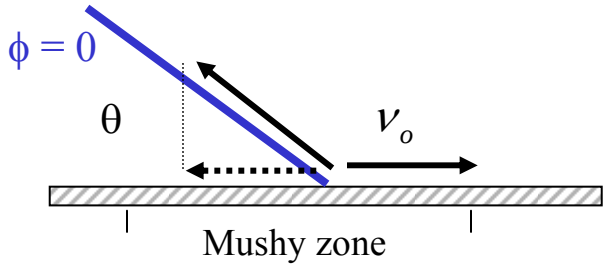

Three unknowns $\begin{cases} v_o \\ \cos\theta_\infty \\ \gamma \end{cases}$ which can be functions of the can be fit to goniometer wetting experiments

3D Computational Model

No penetration / no slip, except near contact region

Outflow occurs at edges of mold chamber

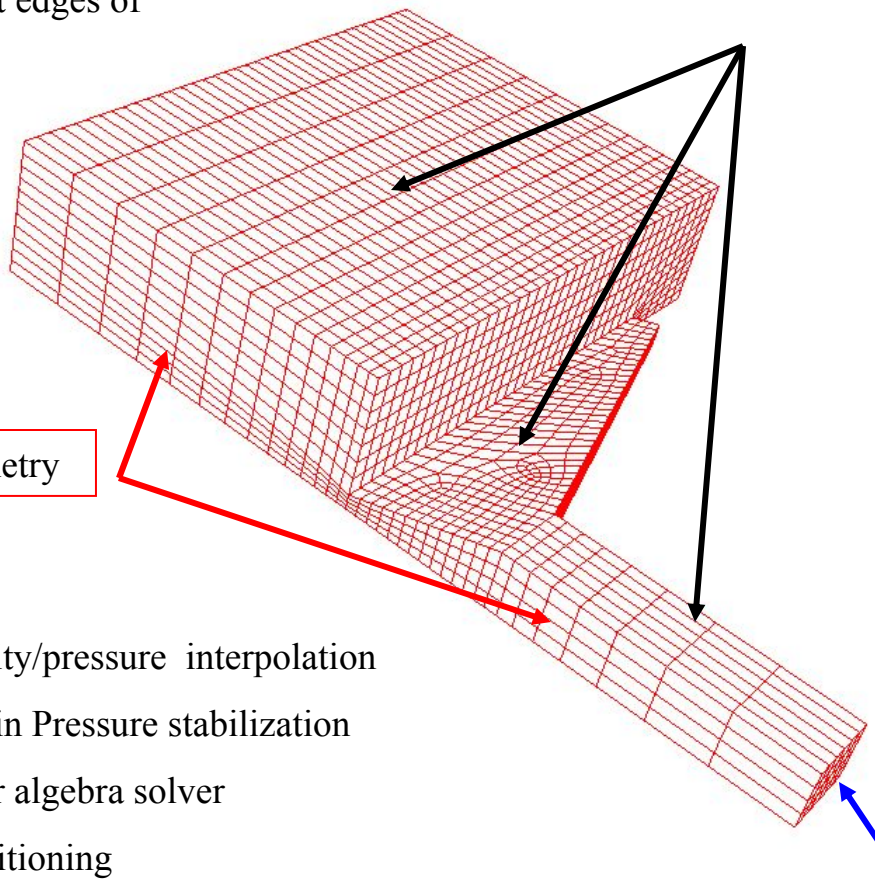

Centerline Symmetry

Flow In

Parameters:

ρ_{liq} = 1.1 g/cm^3
ρ_{gas} = 0.0011 g/cm^3

Newtonian

μ_{liq} = 390 P
μ_{gas} = .4 P

σ = 42.4 dyne/cm

- Bilinear velocity/pressure interpolation
- Petrov-Galerkin Pressure stabilization
- GMRES linear algebra solver
- ILUT preconditioning
- 6744 8-Node hexahedral elements
- 41300 total degrees of freedom

3D Newtonian Model Gives Insights into Distributor Design

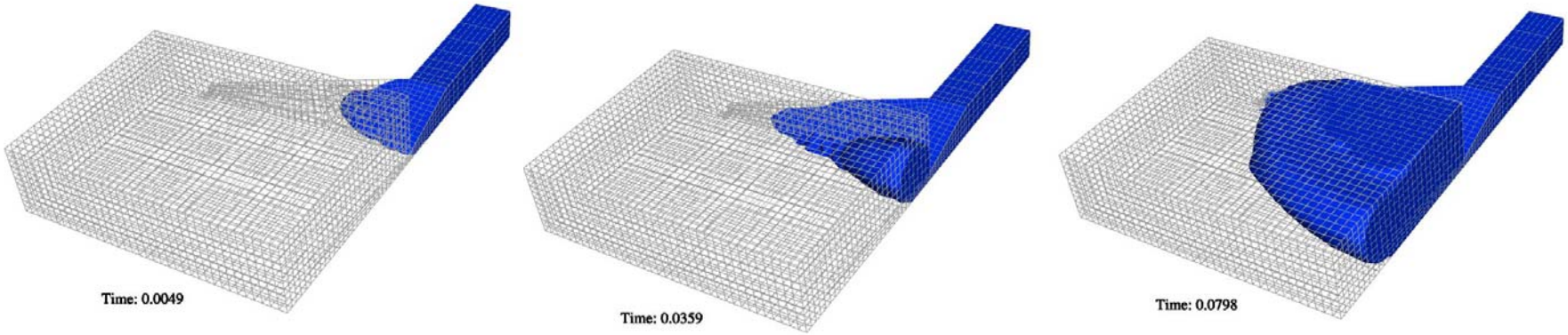

•To minimize mass loss, small amounts of pressure stabilization are used. Matrix is poorly conditioned, requiring GMRES with ILUT fill factors of 3

•Simulation ran for several months on four processors of a Linux HP workstation

•Fluid enters main cavity before completely filling the distributor

•Fluid pools in center of the cavity

•Redesign of distributor may help flow be more uniform

Short shot at 140°C, 100% speed, 50% pressure, 75% fill

Geometry Evolution: Redesign of the Distributor

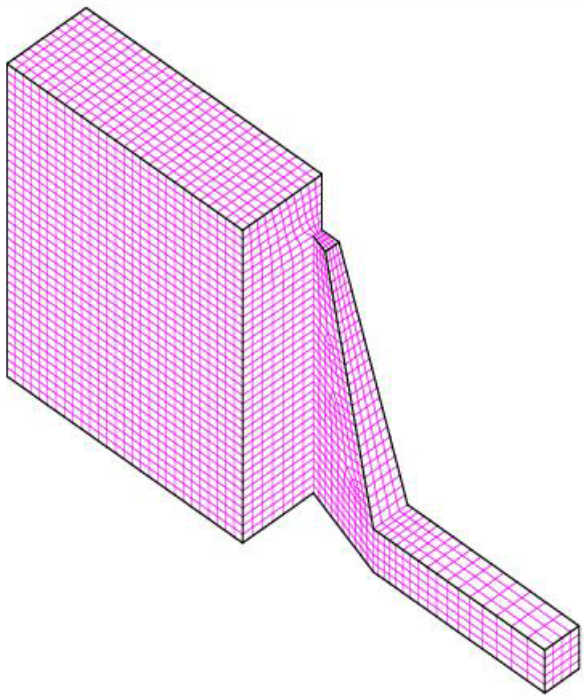

Original Geometry

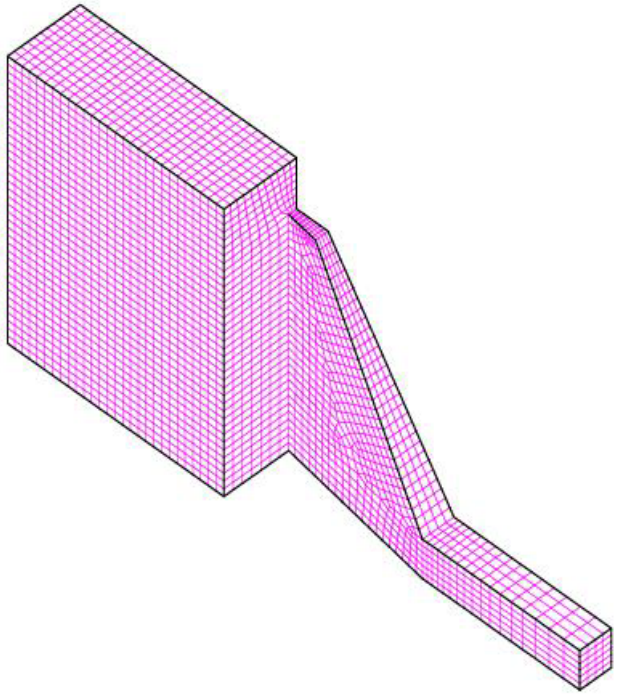

Longer Distributor

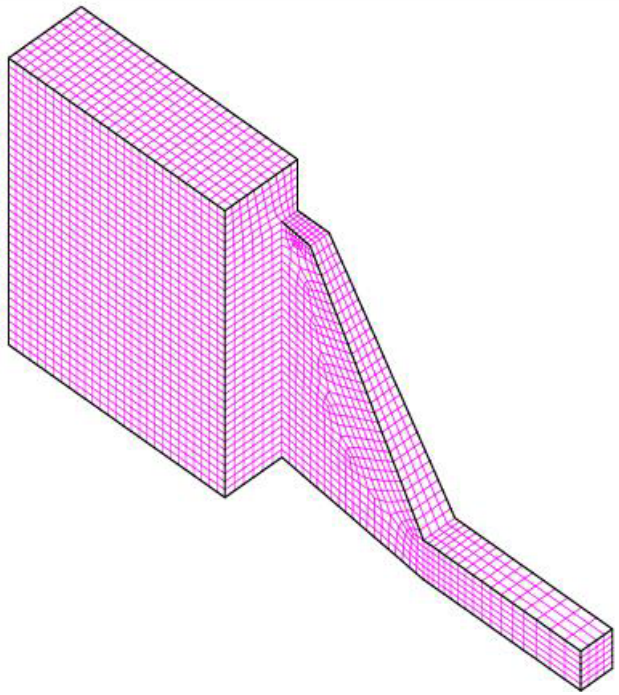

Longer-Taller Distributor

Comparison to Experiment

Vertical Alignment

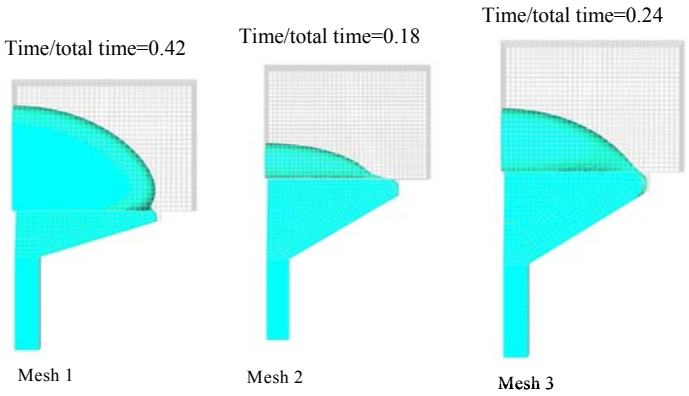

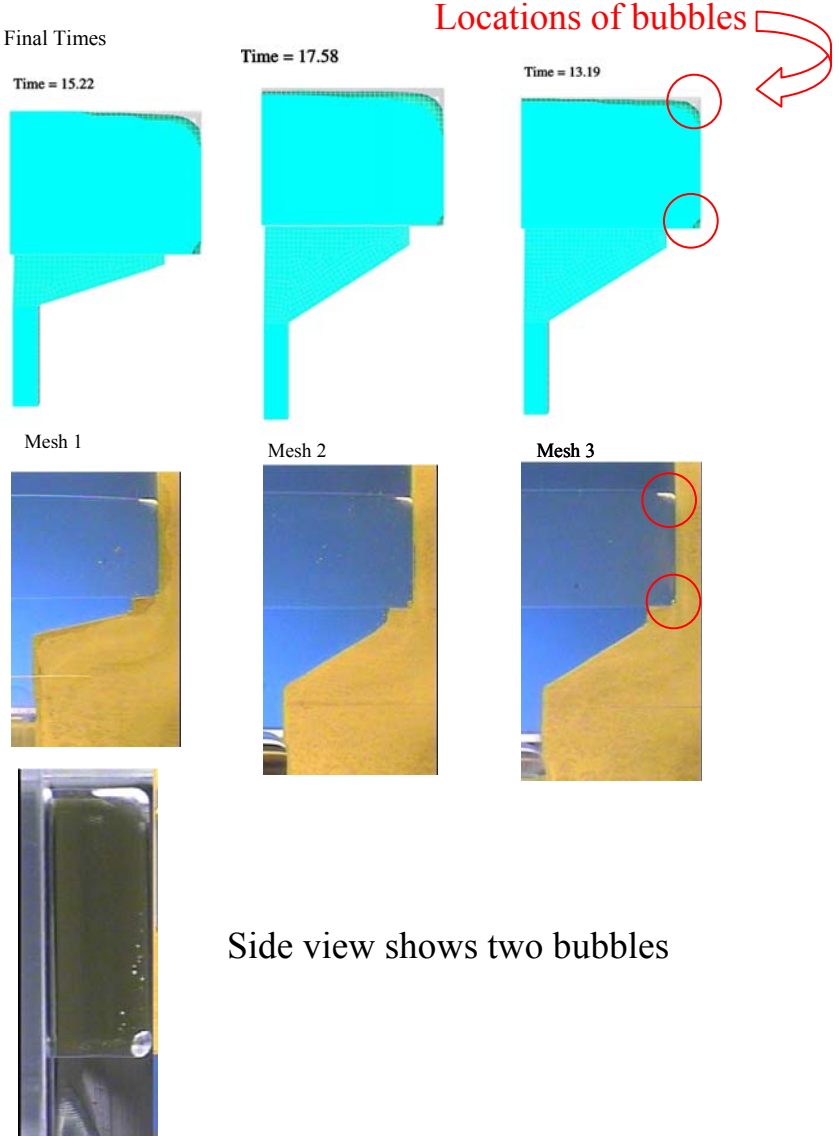

- Qualitative aspects captured – improvements in distributor and number and location of bubbles
- Increasing wetting speed from that measured improves shape of front
- Measured wetting line speed outside of range of goniometer data

Side view shows two bubbles

3D Level Set Model of Mold Filling Compared to Experiment

Model parameters: μ = 390 Poise, θ^{eq} = 39.8°, v_o = 0.0026 cm/s, σ = 42.4 dyne/cm
fill time=14 s

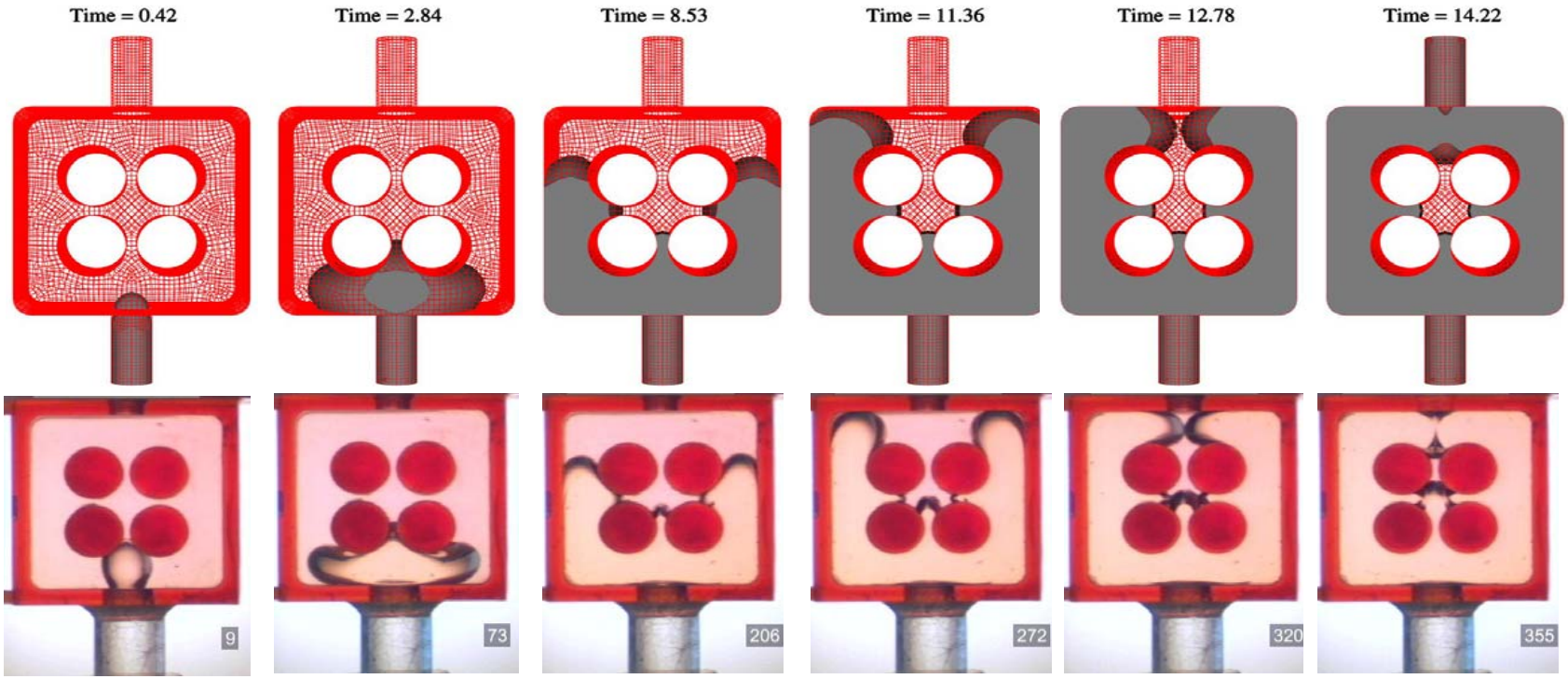

Real parameters: μ = 390 Poise, θ^{eq} = 39.8°, v_o = 0.0013 cm/s, σ = 42.4 dyne/cm
(Ucon 95-H-90000 measured parameters); fill time=12 s

Both: Ca ≅ 20; Re ≅ 0.001

Time*=time/total time

3D Effects

- **Some air escapes as it continues to rise after flow stops**
- **Bubbles remain on back and front walls near outflow**

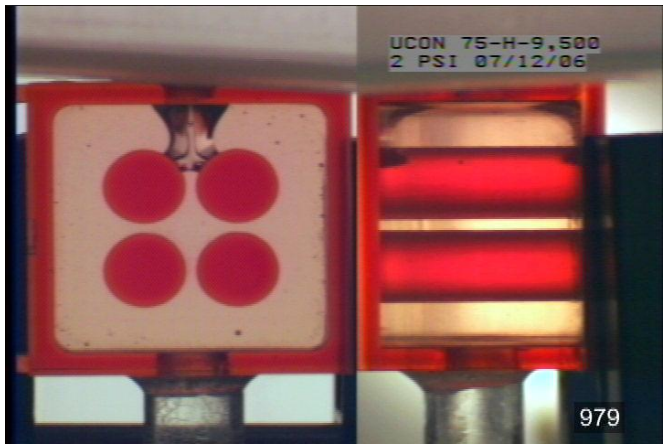

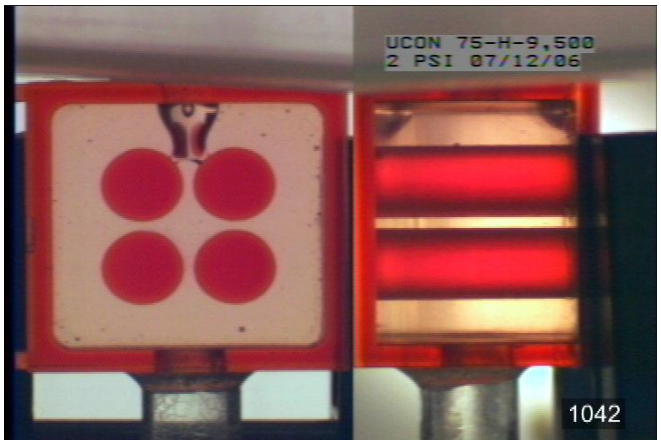

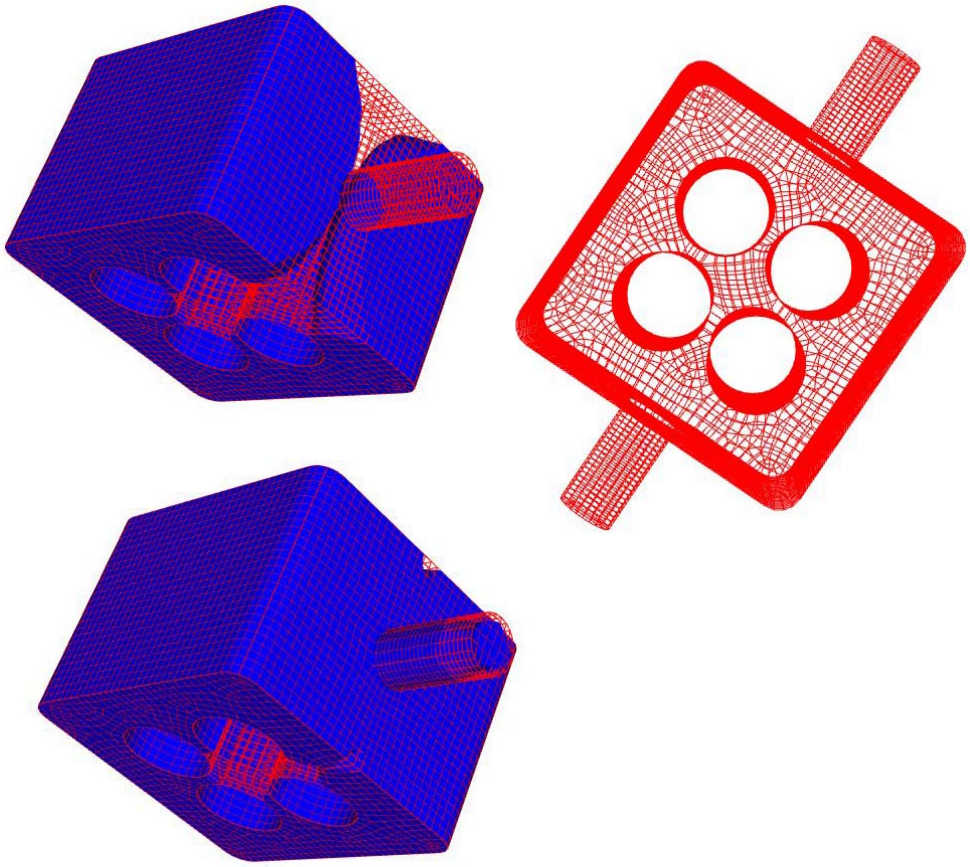

Change of Injection Point: 3D Model With Same Parameters as Experiment

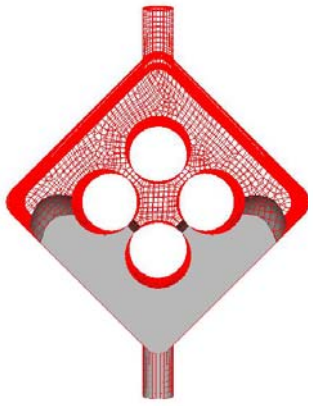

Time*=0.42
Time=10.5

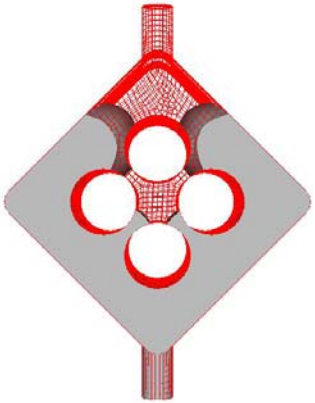

Time*=0.75
Time=18.75

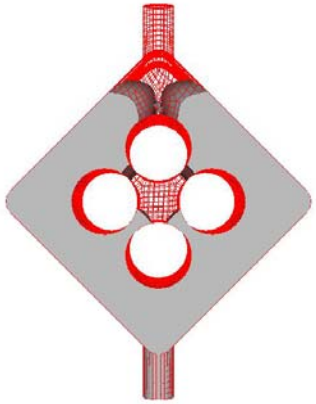

Time*=0.83
Time=20.75

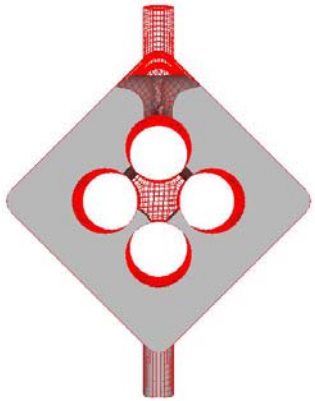

Time*=1.0
Time=22.0

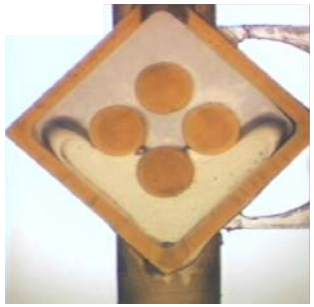

Time*=0.42
Time=5.83

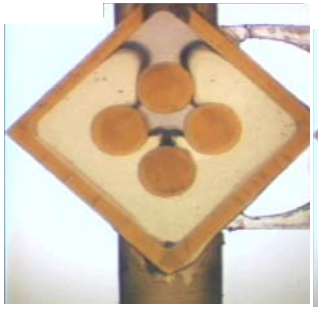

Time*=0.75
Time=10.23

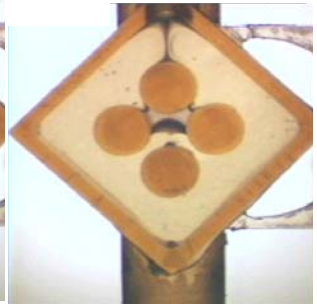

Time*=0.83
Time=11.43

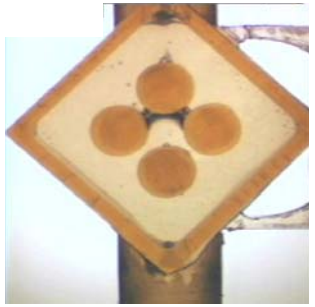

Time*=1.0
Time=13.7

Bottle Filling Capability at Sandia

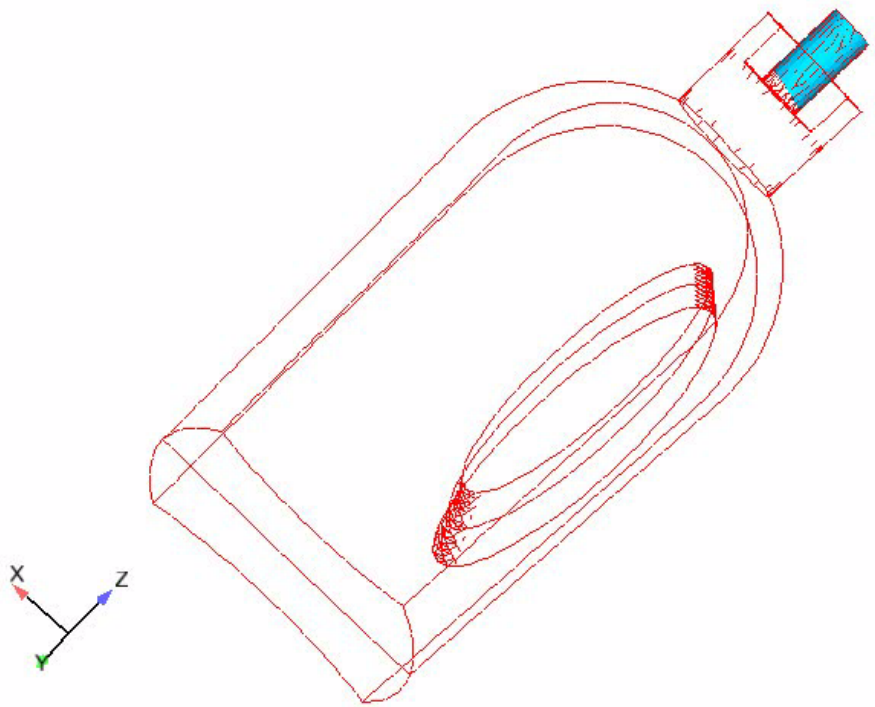

New development effort may improve performance

- ♦Pressure formulation
- ♦Stabilization method
- ♦Curvature projection
- ♦Conformal decomposition finite element (CDFEM) capability for dynamic, sharp interface
- ♦Segregrated algorithms
- ♦Control volume finite element formulations for flow and level set

Method currently conserving mass well, but needs to be faster

Conclusions and Future Work

- Coupled finite element/level set method can be used for modeling mold filling processes and suspension flows
- Results from simulations compare well to experimental validation data, though modeling over predicts void size and underpredicts wetting speed
- Sharp interface methods should improve accuracy of simulations
- Choice of stabilization method depends on Capillary number of regime and importance of surface tension and curvature
- Future work will explore improved algorithms for coupling free surface flow to complex rheology

Viscoelasticity in GOMA

Current Capabilities

- Constitutive equations
  - Maxwell, Oldroyd-B, Giesekus, Phan-Thien Tanner
  - White-Metzner currently disabled.
- Algorithms
  - Elasto-viscous stress splitting/Streamline upwind Petrov-Galerkin
  - Continuous stress
  - Velocity Gradient projection for EVSS
  - Discontinuous Galerkin method for stress with full Jacobians
  - Adaptive viscosity to boost convergence
- Multimode
  - Up to eight stress modes possible